PHILOSOPHICAL TRANSACTIONS OF THE ROYAL SOCIETY A MATHEMATICAL, PHYSICAL & ENGINEERING SCIENCES

The 1995 Bakerian Lecture: Composite Materials

Anthony Kelly

Phil. Trans. R. Soc. Lond. A 1996 **354**, 1841-1874
doi: 10.1098/rsta.1996.0081

The 1995 Bakerian Lecture
Composite materials

By Anthony Kelly

Churchill College, Cambridge CB3 0DS, UK
and Department of Materials Science and Metallurgy, University of Cambridge, Pembroke Street, Cambridge CB2 3QZ, UK

Contents

Examples of engineering artefacts made with modern composite materials are given, followed by a brief discussion of the range of physical properties attainable by fibre composites. Physical properties are usually simply additive but the strength properties are not. Multiple fracture is discussed in detail to show how cracks can be used to confer microductility and to provide energy absorbing structures.

This opens the way for the use of ceramic materials as high temperature substitutes for metals. A possible microstructure for very high temperature creep resistance is discussed in detail; it consists of alternate layers of single crystals of differing lattice constant and elastic modulus.

Finally the concept of a smart material is discussed showing how structures may be monitored with fibres and their mechanical response controlled or modified.

1. Introduction

President, Your Royal Highness, Ladies and Gentlemen...

The growth in importance of composite materials over the past 35 years since the invention of strong and stiff boron fibres in 1959 (Talley 1959) and of carbon fibres a

Phil. Trans. R. Soc. Lond. A (1996) **354**, 1841–1874
Printed in Great Britain

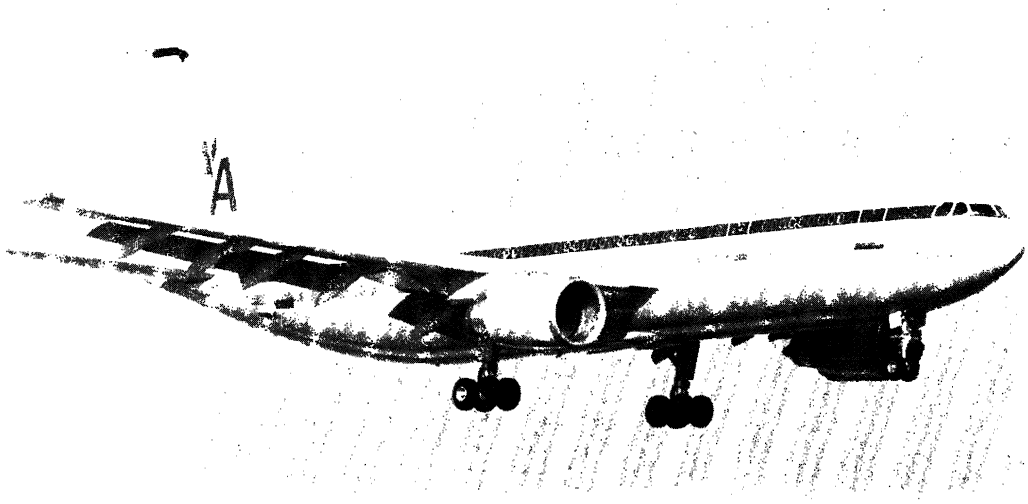

Figure 1. The Airbus A300-600, contains many components made of composites; the entire rudder and fin, engine cowlings, radome, large sections of the tailplane; the air brakes, spoilers, outer flap and wing tip, and undercarriage doors.

few years later (Watts *et al.* 1964; cf. also aramid fibres (Kwolek 1968)) is a wonderful example of the synergy possible between engineering and predictive science.† The science is principally that of the relationship between structure and properties of solid or near solid material, while the engineering encompasses the processing and manufacture of composites and the design of them into new structures: some chemical and much mechanical engineering.

This account of composites is written by one interested in the science of materials; in *predicting* not just describing how solid materials behave under the action of mechanical and sometimes chemical forces mainly in a terrestrial environment. Several recent artefacts made with fibrous composite materials are shown in figures 1–4. These illustrate that modern fibrous composite materials are used in a wide variety of engineered structures.

2. Composite properties

(*a*) *Physical (and chemical) properties of composites*

The conventional description of a composite is of a multicomponent material designed to achieve a combination of physical properties. That is a good description and the behaviour of composites thus viewed will form the basis of this lecture. However, there is another thought engendered by thinking of composite materials which is to use the composite as a means of carrying out a synthetic process and I will briefly deal with this first.

Birchall (1983) has described the use of a processing aid in the production of macrodefect-free cement. Newkirk *et al.* (1986) ingeniously allow the oxidation of,

† For the material in § 6 we note that fibres for optical communication over long distances (many kilometres) were developed a little later, in the early 1970s. In the mid 1970s it was found that losses are very low at particular wavelengths e.g. 1.3 μm (Payne & Gambling 1975).

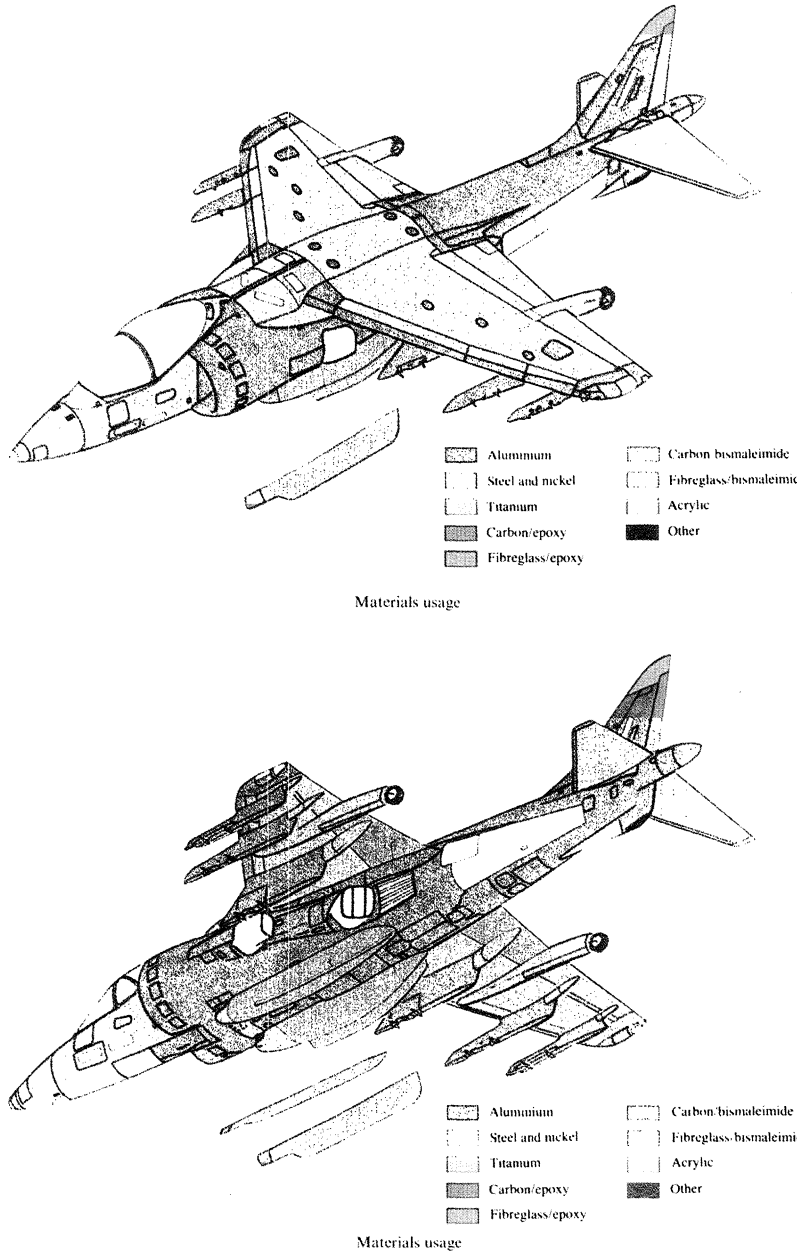

Figure 2. The Harrier aircraft illustrating that many components are made of composites – multimaterials rather than single materials; from Riley (1986).

say aluminium, to aluminium oxide to produce a composite of silicon carbide within an aluminium oxide matrix; first infiltrating the mass of fibrous SiC with aluminium and allowing this to oxidize. The aluminium is lost in the process as is the rheology aid in Birchall's cement. (Kelly (1990) describes some other examples.)

The intractable chemistry of the lighter (Si, Be, B, C, N) non-metallic elements

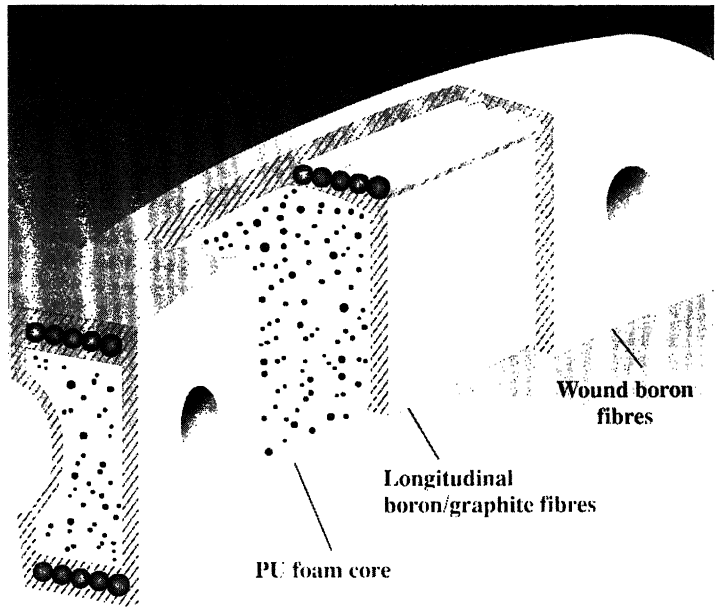

Figure 3. Cross section of a modern high technology tennis racket.

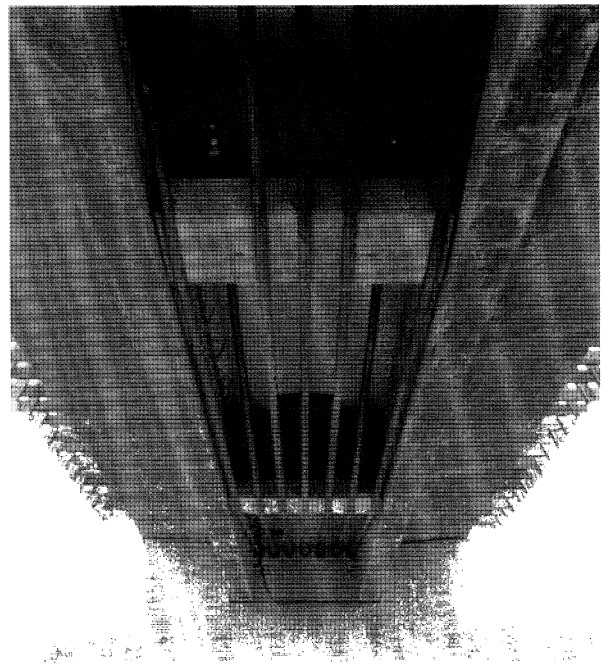

Figure 4. The Marienfelde Bridge in Berlin showing the use of external grp reinforcing tendons.

and their compounds which do not melt or which resist solvation can be overcome so as to produce new and hitherto unobtainable compounds, e.g. $SiBN_3C$, by a sort of composite fabrication process whereby a fibre is spun first and is then pyrolysed or otherwise treated to produce the required, or almost the required, combination

of the light elements. This approach was pioneered by Yajima (e.g. Yajima 1980) to produce fibres with composition (roughly) equivalent to SiC. Lately Baldus and his coworkers have produced quite new compounds such as the one cited and others from a single relatively cheap precursor $Cl_3Si–NH–BCl_2$. Fibres produced by pyrolysis have high modulus and strength at room temperature and, it is claimed, very high oxidation resistance at temperature greater than 1500 °C, thus rivalling oxides at this temperature (Baldus & Passing 1994).

Exploration of the general physical properties of binary composites has not developed as a very exciting field (Hale 1976; Albers 1986; Newnham 1994). Generally the properties of the composite lie between those of the two components and often a weighted average by volume of the two components is quite sufficient to predict a given property (density, electrical resistance, specific heat). Since fibres are often used, the composite may be highly anisotropic but even so the properties in particular directions are still adequately given by appropriate weighted averages (elastic modulus, thermal conductivity, etc.). Other physical properties are dealt with by Hale (1976).

Although there are very few surprises, some among the thermomechanical properties are quite striking: e.g. negative thermal expansion coefficient (Ashton *et al.* 1969) and negative Poisson ratio both in plane (Tsai & Hahn 1980) and through the thickness (Herakovich 1984). This last can be quite useful, e.g. when dome shaped objects are required to be produced by bending, since a negative Poisson ratio will avoid anticlastic curvature (Evans 1990). In addition a smooth variation of physical property can be obtained, see figure 5, which is useful in matching components, e.g. glass to metal seals or in prosthetic devices. Matching of acoustic inpedance at interfaces is also a very useful advantage. Sometimes there can be cases where a well-known physical property has a value lying outside that shown by either component; an example is acoustic wave velocity see figure 6. Useful compilations of the formulae for evaluating the thermomechanical properties of composites are given by Schoutens & Zorate (1986) and by Ashby (1993); care needs to be taken over typographical errors.

(*b*) *Mechanical properties of composites*

Some of the simpler mechanical properties, e.g. longitudinal strength of an aligned composite or even compressive strength (Kelly & Tyson 1965) vary linearly with volume fraction when the strength of the fibres is itself a well-defined number, and the breaking strain of the two components is the same (Mileiko 1969). However, in general, the strength properties are very far from additive. A fascinating example of this non-additivity is afforded by the very creep resistant alloys with which ceramic matrix composites may soon be in contention for use as very high temperature resistant materials. Figure 7 shows the minimum creep rate as a function of stress at 600 °C for pure nickel, for a range of nickel chromium (solid solution) alloys called γ and for Nimonic 80 A which contains γ^1 ordered alloy (of $Ni_3(Al,Ti)$) in a γ matrix and for γ^1 itself. It is clear that the 'composite' shows much greater resistance to creep than does either the γ or γ^1 component (McLean 1995).

This is a striking example from metallurgy where the non additivity of properties and hence the enormous synergy depends for its explanation upon the properties of dislocations within the material.

In a homogeneous material and in many single-phase materials the behaviour of the dislocations and of the cracks does not depend upon the atomic structure at the

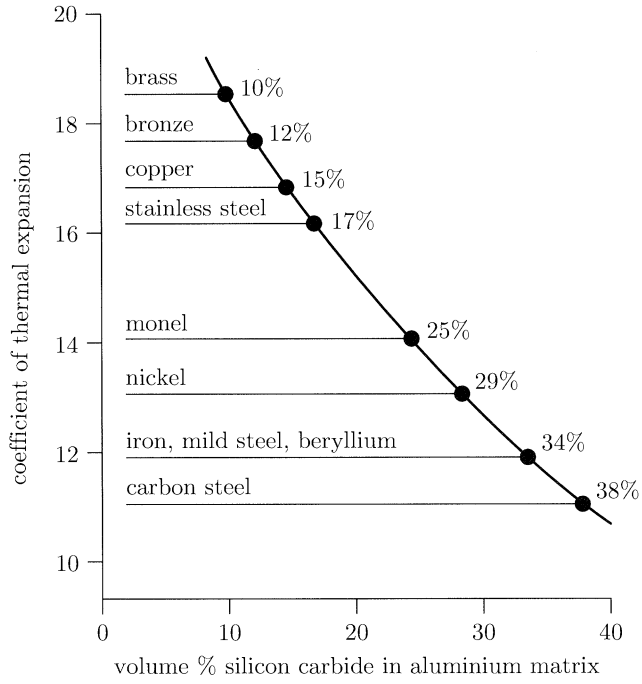

Figure 5. Variation of the thermal expansion coefficient of a composite of aluminium with the indicated volume fraction of silicon carbide particles. The ordinates are in units of 10^{-6} K^{-1}.

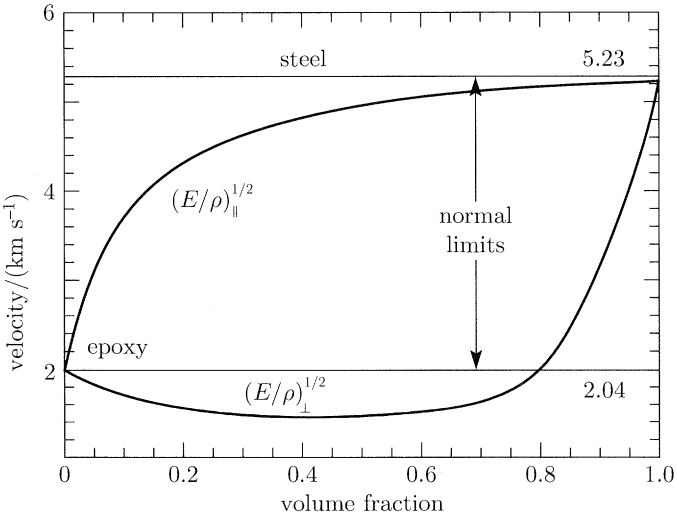

Figure 6. Plot of the acoustic wave velocity, parallel to the fibres $(E/\rho)_{\parallel}^{1/2}$ and normal to the fibres $(E/\rho)_{\perp}^{1/2}$ versus volume fraction for aligned steel fibres in epoxy resin. The Young's modulus of the steel wires is 220 GPa and the density 7.9 Mg m^{-3}; of the epoxy 5 GPa and 1.2 Mg m^{-3}, respectively.

dislocation core or at the crack tip. Since one leads to flow and ductility and the other is first encountered in brittle materials (cracks in glass), the similarities between the

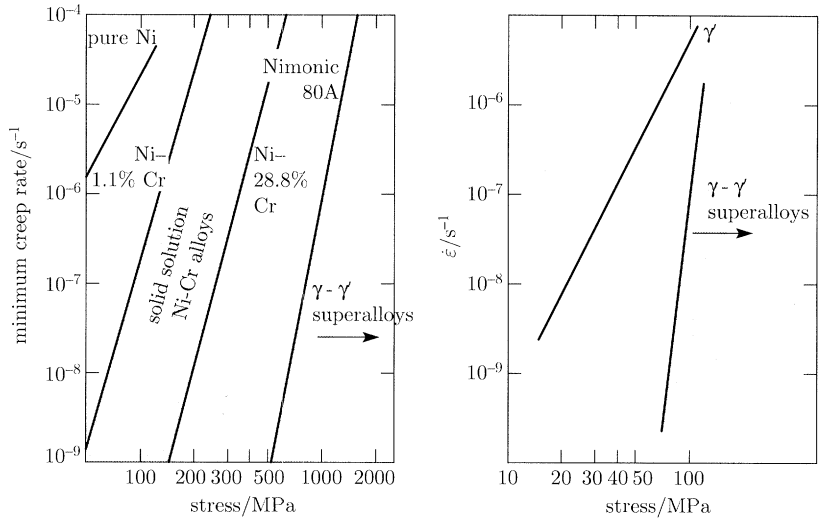

Figure 7. Plot of the measured minimum creep rate as a function of stress at 600 °C for nickel, nickel–chromium solid solution alloys and for Nimonic 80A, γ–γ^1 superalloy (left-hand diagram). The right-hand diagram shows a comparison, this time at a higher temperature (980 °C) for single crystal $\langle 100 \rangle$ oriented Ni_3Al (γ^1) and of a directionally solidified γ–γ^1 superalloy; from McLean (1995). The γ–γ^1 superalloy is more resistant to creep than is either component.

two defects are often overlooked. This is compounded by the fact that a distinction is not clearly drawn between a crack and a notch. However, the main mechanical principles governing the motions of a group of dislocations (pile-up) and of a crack are very similar (Friedel 1956; Hirthe & Lothe 1968) and in any real material composed of atoms, the nature of the core of the dislocation and of the tip of the crack both require detailed knowledge of the binding forces between atoms at large strains and the form of the core or tip becomes a property of the specific material. The similarities between a crack and a dislocation and their intimate connection are explained in more detail in § 2 *c* below.

At temperatures below that at which diffusional flow occurs dislocations control the flow and fracture of ductile metals and to some extent the mechanical properties of crystalline polymers. The strength properties of brittle things are dominated by the properties of cracks.

Composite science has enabled us to control and influence the properties of cracks in brittle things (Aveston *et al.* 1971) and enable the engineer to consider seriously the use of brittle materials in engineering structures.

The phenomenon of multiple fracture which is dealt with in § 3, imparts a type of useful ductility to composites composed of two fully brittle materials. It is because of the phenomenon of multiple fracture and the possibility of engineering sufficient energy absorbing capability, as well as the capability of sufficient local load redistribution around a notch, that all brittle systems are now considered for practical application. A particularly important aim is the production of a very strong material able to extend the temperature regime to much higher temperatures in air under which engineers may operate.

The attainment of this goal involves much of materials science and it excites me personally at present. How such may be achieved emphasizing, where appropriate, composite principles is dealt with in § 5. A final section of this lecture deals with possible methods of monitoring the performance of composites in service.

(c) The crack and the dislocation

The crack and the dislocation are, respectively, the most important planar defect and line defect in solids, whether the solid be crystalline or amorphous. The detailed behaviour of each in a particular solid is governed by the atomic structure of the tip and of the core respectively, though rather general rules of behaviour apply to each regardless of the atomicity. The detailed nature of the tip and of the core structure is important in answering the question whether, under given conditions of strain rate and temperature and other physical factors, a solid will be ductile or will break in a brittle fashion (Thomson 1994).

The stresses close to the tip of a crack in a solid under stress are determined by the interatomic forces holding the body together and the geometric form of the tip is a property of the material. They may not be directly measurable for the reasons given by Kendall (1994), and well investigated experimentally, when clean smooth surfaces are brought into close contact. In fact a true crack under stress is in unstable equilibrium. Its tip moves in a discreet and non-continuous structure; an analagous situation arises in the case of a dislocation where it has long been recognised that the most important manifestation of lattice periodicity is the generation of a dissipative friction stress known as the Peierls–Nabarro stress which impedes dislocation motion. The corresponding effect with the crack is that it can become lattice trapped over a range of lengths (Thomson *et al.* 1971) because the energy required to form its surface must include a finite structure term having the periodicity of the lattice (or of the average interatomic distance in a glass). In full detail then, the fracture process becomes thermodynamically irreversible because the crack must grow unstably between positions of maximum and minimum energy in the fine structure term.

Examination of modern models of the crack tip show that the fracture mechanics parameters governing lattice trapping exhibit the same very sensitive dependence on the width of the crack front as does the Peierls–Nabarro stress upon the width of a dislocation core (see, for instance, the book on dislocation dynamics (Rosenfield *et al.* 1968)). The relationship between crack and dislocation becomes even more intimate when it is realized that in strongly directionally bonded crystals, when the Burgers vector of the dislocation is a good deal greater that the separation of nearest neighbours as in the diamond structure, the dislocation core contains a crack of atomic dimensions.

When macroscopic cracks and large numbers of dislocations are involved these atomic considerations appear very recondite but the atomic nature of the crack tip does govern slow crack growth in many ceramic materials and governs the important phenomenon of static fatigue.

Fracture mechanics, the science and engineering of controlling cracks usually demands that plastic flow be invoked in order to inhibit crack growth. In a metal the crack is regarded as the defect to be avoided at almost any cost. One view of the composite is that the well-designed composite actually uses cracks and far from merely rendering them harmless, encourages their formation in certain cases.

3. Multiple fracture

Figure 8 shows the stress–strain curves in tension of two materials both commercially available. The dotted curve is that of a glass without fibres and the second the same initial material plus fibre with the composite strained parallel to these. The

PHILOSOPHICAL TRANSACTIONS OF THE ROYAL SOCIETY A MATHEMATICAL, PHYSICAL & ENGINEERING SCIENCES

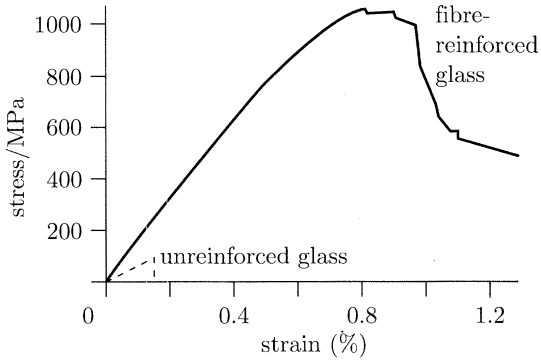

Figure 8. Stress–strain curves of a commercially available composite material consisting of 40% aligned carbon fibres in a borosilicate glass (full curve); and of the glass alone (dotted curve).

result is a striking difference. The fact that the stress–strain curve in the second is not linear to fracture implies a type of ductility in the specimen. This is an example of a specimen undergoing multiple fracture. Multiple fracture is of very widespread occurrence, and occurs in situations as diverse as the cracking of a brittle lacquer on a ductile metal when the latter is extended, and the cracking of carbide whiskers in a eutectic within a nickel base alloy when a specimen is extended in tension. In both cases as the specimen is extended the surface becomes covered with an array of parallel cracks. The cracks are only at the surface in the case of the brittle lacquer. In the case of the carbide whiskers, each whisker is seen to be broken into a set of short lengths. The phenomenon is sometimes called transverse cracking, when it occurs in laminates. It arises whenever one component in a multicomponent system breaks at a smaller strain than the other and there is sufficient of the high elongation component so that it is able to bear the total load which is then thrown upon it in a tensile test.

So, for instance, if a 0°–90° balanced laminate is strained in tension and there are sufficient of the 0° plies as is most often the case, then, after quite a small strain of the same order as the transverse failure strain in a single ply, the specimen is found to contain a set of parallel and closely spaced cracks within the 90° ply. Bailey *et al.* (1979) give a beautiful set of examples.

The phenomenon was first named multiple fracture by Cooper & Sillwood (1972) and was initially extensively investigated in cement matrix composites by Aveston *et al.* (1971), who described the essentials of the process and also dealt with the effect of the cracking on the stress–strain curve. A review of multiple fracture in laminated composites has been given by Abrate (1991) and many beautiful pictures published (see, for example, Allen 1994). The understanding and control of the effect is of great importance for the use of laminated composites since the array of cracks lowers the longitudinal modulus, and alters Poissons ratio and the thermal expansion coefficient. It has likewise a very important effect on fatigue properties (see, for example, Talreja (1987) for a fine review) and, of course cracking can be induced by changes of temperature.

The effect is also of very great importance in composites with a ceramic matrix which are designed to be used at elevated temperature since on the one hand cracking of the matrix can provide ductility but it can also allow the ingress of gases which leads to oxidation of the fibres or other injurious reaction. Matrix cracking of much

PHILOSOPHICAL TRANSACTIONS OF THE ROYAL SOCIETY A MATHEMATICAL, PHYSICAL & ENGINEERING SCIENCES

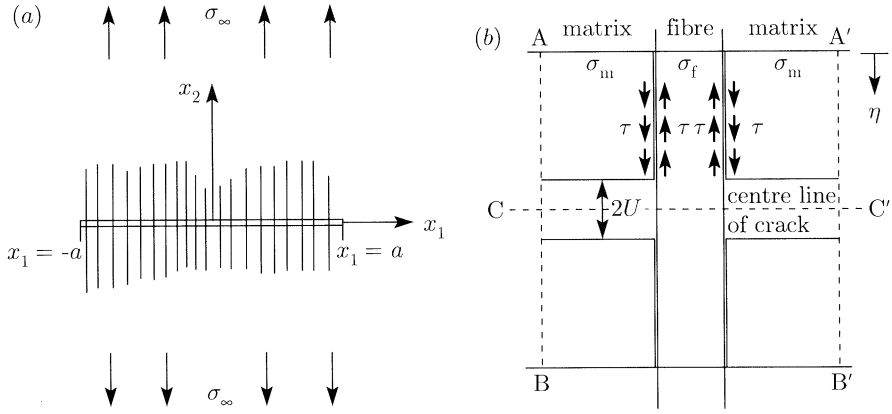

Figure 9. (*a*) Schematic diagram of a matrix crack in a uniaxially aligned fibre composite. (*b*) Schematic diagram of the crack opening resulting from matrix cracking followed by debonding at the fibre–matrix interface. $2U$ is the opening of the crack; from McCartney (1987). The notation is the same as that in figure 13.

the same type, though on vastly different scale of size is also important in normal reinforced concrete.

Cracking may be reduced by making the 0° plies thinner in a laminate or by decreasing the diameter of the fibres in a unidirectional specimen; decreasing the diameter of the fibres also reduces the inter-fibre spacing for a given volume fraction of fibres.

This effect has been explained either by using an approach based on the energetics of the process of cracking (Aveston *et al.* 1971; cf. also McCartney 1987) see below, or as a result of statistical variation of the strength whereby thinner things are stronger (Manders *et al.* 1983).

Whether or not matrix cracking occurs is a central question in the utilization of ceramic matrix composites. The state of crack envisaged is shown in figure 9, where it is made clear that 'debonding' between fibre and matrix must be taken into account. If there is no debonding the crack may penetrate the fibres.

The parameters involved in describing the behaviour of such bridged cracks are then those describing the distribution of fibres and their properties (volume fraction V_f, radius, work of fracture, Young's modulus E_f, Poisson's ratio ν_f) those of the matrix E_m, ν_f work of fracture, etc., and in particular the assumed value of the cracking stress of the matrix in the absence of fibres, and parameters depending on both components properties, i.e. an interfacial shear strength τ and a debonding energy γ_{db}. These parameters are related to the crack spacing at equilibrium which is attained if the loading of the specimen is continued to strains much larger than that at which the set of parallel cracks first forms within the matrix. In any particular system it must not be assumed that under zero imposed load both matrix and fibres are unstrained; there are usually residual strains present resulting from the fabrication.

There have been many detailed analyses of the experimental situation particularly by Evans and his school (Evans & Zok 1994; Evans 1996), who, following pioneering work by Prewo (1982), has developed an enormous body of useful knowledge for the engineer. Figure 10 shows that some of the necessary parameters can be deduced from the analysis of hysteresis found on loading and unloading in uniaxial tension (Pryce & Smith 1993).

PHILOSOPHICAL TRANSACTIONS OF THE ROYAL SOCIETY A MATHEMATICAL, PHYSICAL & ENGINEERING SCIENCES

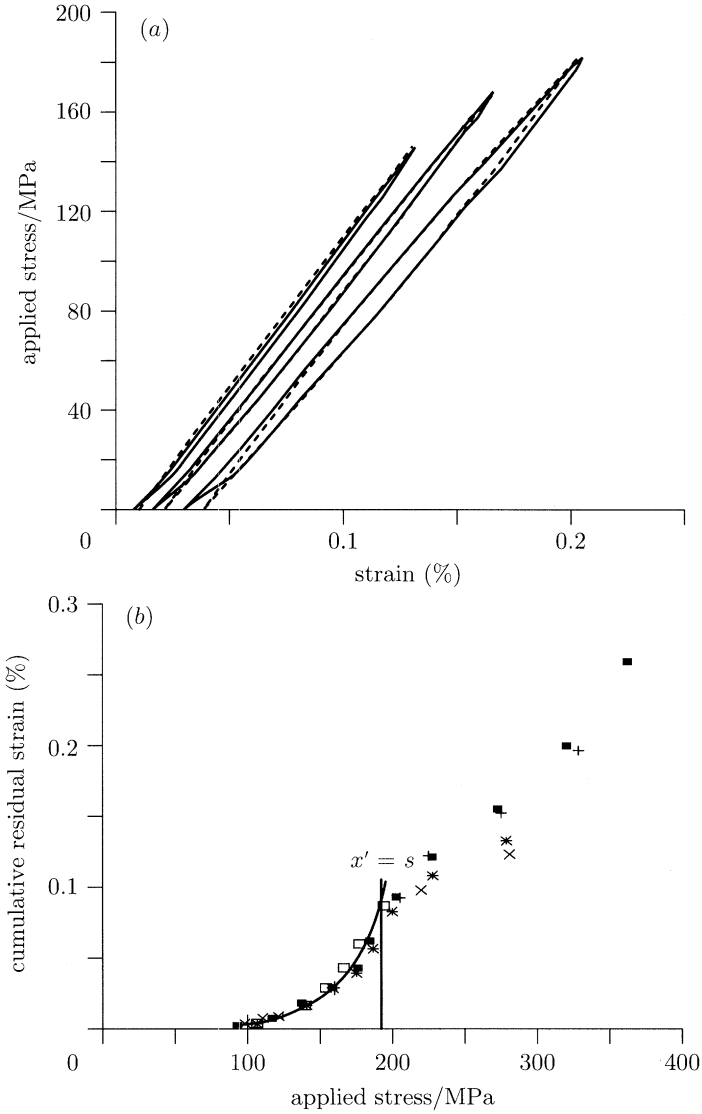

Figure 10. (*a*) Stress–strain hysteresis loops obtained by cycling unidirectional SiC–CAS laminates containing a volume fraction of 0.34 of Nicalon fibres; comparison of prediction, dotted, and experiment. (*b*) Plot of cumulated residual strain versus applied stress for specimens as in (*a*), cycled up to various strain levels together with model predictions based on a value of shear strength of 14 MPa and a value of thermal stress of −173 MPa, full line. To the right of the line $x' = s$, the fibres slip through the matrix. Replotted by P. A. Smith from Pryce & Smith (1993).

When the cracks can be assumed to be very regularly arranged, as in a 0°–90°–0° cross ply laminate, McCartney (1992) derives exact expressions for the longitudinal Young's modulus, Poisson's ratio, transverse Young's modulus and thermal expansion coefficient as a function of the density of cracks. These arrays of cracks are the principle means of conferring acceptable toughness upon all brittle load bearing systems so that the engineer can have confidence that in a highly critical component, should failure occur by overloading, then a benign (not sudden and catastrophic) failure will result. The required type of stress–strain curve is well illustrated in fig-

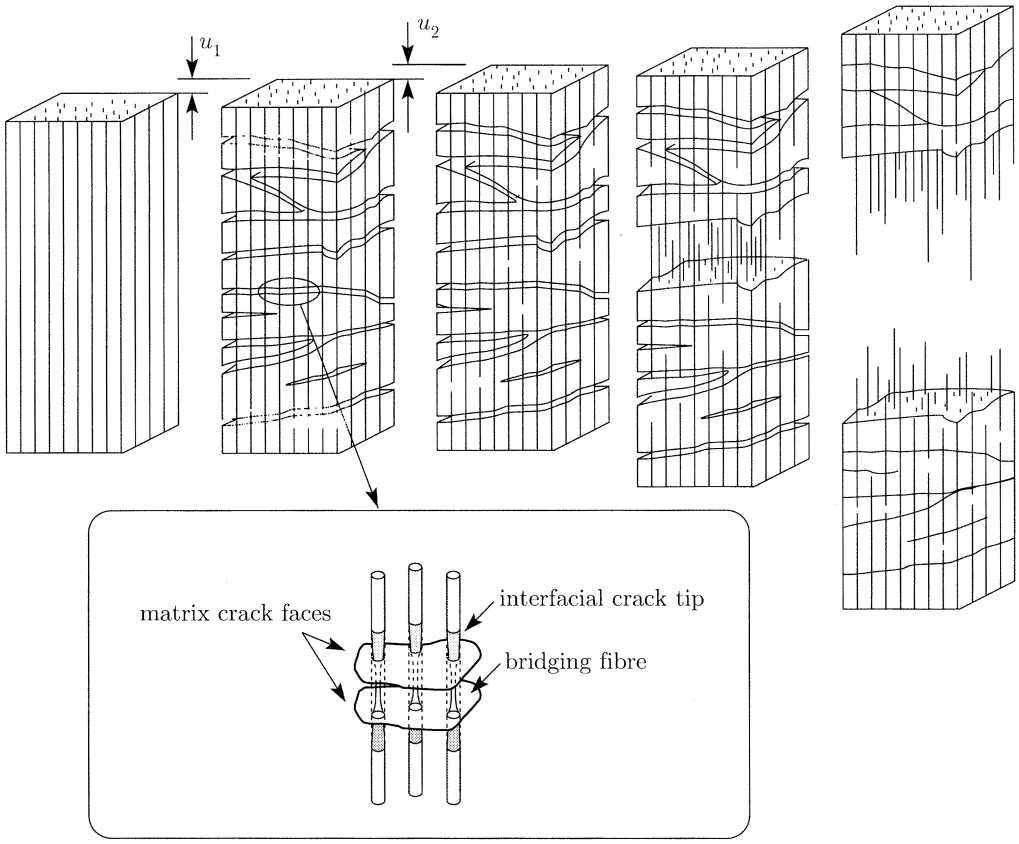

Figure 11. Schematic diagram of the effects accompanying tensile straining of a fibre reinforced brittle matrix material. On the left hand side the matrix and fibre will be subject to the same elastic displacement u_1. When multiple fracture first occurs the fibres extend further to u_2, and the fibres and matrix 'debond'. Thereafter fibres may break and eventually sufficient are broken for total failure by two halves of the specimen pulling apart; far right hand. As the stress on the fibres is relieved the cracks in the matrix will partially close.

ure 8 where the fibre reinforced glass continues to show considerable extension after the peak stress is passed.

The form of the stress–strain curve followed by either a single lamella or a 0°–90°–0° laminate containing many fibres is similar and it is followed whether the aligned high elongation (high strength) fibres are continuous or discontinuous. The matrix first fails and is traversed by a set of parallel cracks. These provide the non-elastic displacements which allow the specimen to extend. The failure of the individual fibres will not lead to failure and some fibre failure may occur on a rising stress–strain curve. The ultimate strength is governed by the bundle strength of the fibres and after the UTS is reached final separation into two or more pieces occurs by pullout. These effects are shown schematically in figure 11.

The multiple cracks provide a form of energy dissipation, and in all brittle systems this is almost the only major one. A striking form of microductility introduced by cracks is shown in figure 12.

Of course, once such cracking has occurred and if it occurs throughout the body of the specimen, then gases may permeate the whole body. In bending the compos-

PHILOSOPHICAL TRANSACTIONS OF THE ROYAL SOCIETY A MATHEMATICAL, PHYSICAL & ENGINEERING SCIENCES

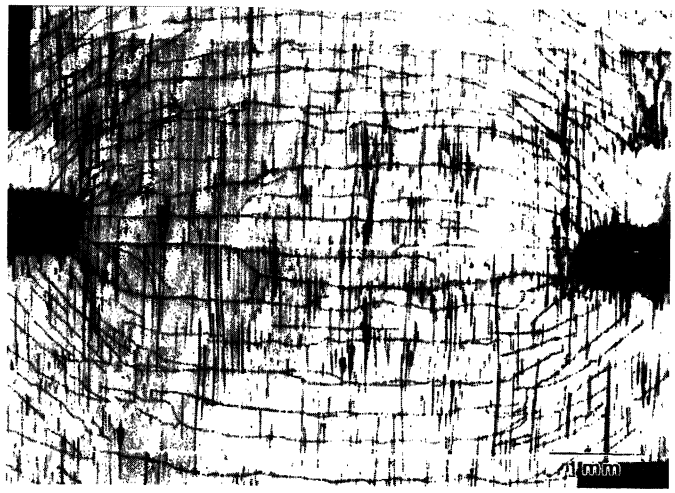

Figure 12. Multiple cracking occurring between two notches in a laminated composite of 16 layers of 0°–90° lamellae each containing 40 vol.% of SiC fibres in a calcium aluminiosilicate glass matrix. Photograph courtesy Carl Cady.

ite material may of course remain gas tight since one side will be in compression. Whether having tension members in a permanently cracked state is a viable engineering proposition remains to be seen. Of course I am emphasizing (as an introduction to § 5 of the paper) multiple fracture in a composite where both components are very brittle. In metal matrix composites and in resin matrix composites tension members need not be permeated by cracks.

The full extent of matrix multiple cracking only occurs, of course, if the specimen is subject to sufficient elongation so that the cracks may be fully opened. It is an experimental fact that cracking of the matrix can be restrained and hence its fracture strain greatly increased. Strain is used rather than stress here because in an unidirectional composite before cracking, strain in the two components in the longitudinal direction is equal and because the stress in the matrix and in the fibre is not the same as the external applied stress.

The theory of how this occurs is interesting because it demonstrates a very complete control of cracking.

If a brittle material of modulus E_{m}, plane strain fracture toughness $K_{\mathrm{Ic}}^{\mathrm{m}}$ contains a volume fraction V_{f} of aligned fibres of circular section, radius r and modulus E_{f}, a pre-existing crack of length $2a$ within the matrix, which is spanned by unbroken fibres, cannot run across the specimen unless the strain energy release rate of the composite exceeds $2\gamma_{\mathrm{m}}V_{\mathrm{m}}$, where $2\gamma_{\mathrm{m}}$ is the work of fracture (twice the surface energy in principle for a completely brittle material) of the matrix. It follows that the fracture toughness of the composite resisting passage of this crack is

$$K_{\mathrm{I}} = K_{\mathrm{Ic}} = \left[\frac{2E_{\mathrm{c}}\gamma_{\mathrm{m}}V_{\mathrm{m}}}{(1-\nu^2)}\right]^{1/2} = \left[\frac{V_{\mathrm{m}}E_{\mathrm{c}}}{E_{\mathrm{m}}}\right]^{1/2} K_{\mathrm{Ic}}^{\mathrm{m}}, \tag{3.1}$$

where ν is Poisson's ratio.

Provided that we always have σ_∞ (the remote stress on the composite) less than $\sigma_{\mathrm{fu}}V_{\mathrm{f}}$, where σ_{fu} is the breaking stress of the fibres (assumed to be constant) then we can model the situation of the fibres crossing the crack and restraining its opening by a non-uniform distribution of pressure on the faces of the crack of opposite sign

to σ_∞. Then

$$K_{\mathrm{I}} = \sigma_\infty \sqrt{(\pi a_0)} Y, \tag{3.2}$$

where Y is a function depending upon the elastic properties, volume fraction and radius of the fibres and the sliding friction between fibres and matrix. McCartney (1987) finds values of Y and hence of K_{I}. By equating K_{I} to K_{Ic} given by (3.1) a master curve is produced shown in figure 13, showing the dependence of the critical stress for matrix cracking $\sigma^{\mathrm{c}}_\infty$ upon the length of a pre-existing matrix crack. The parameters σ_0 and a_0 are related as

$$\sigma_0 \sqrt{(\pi a_0)} = K_{\mathrm{Ic}}. \tag{3.3}$$

It is seen from figure 13 that there is a limiting stress required to expand even the longest cracks and that the curve is monotonic decreasing, so that if a crack starts to expand it runs all the way across the specimen if the applied stress is maintained. The limit corresponds exactly to the ACK limit (Aveston *et al.* 1971). Because for a material without fibres a crack of length $2a$ expands if

$$\sigma^{\mathrm{m}}_\infty = K^{\mathrm{m}}_{\mathrm{Ic}} \sqrt{(\pi a)}. \tag{3.4}$$

we can, using (3.1) and (3.3) express this result as

$$\left(\frac{\sigma^{\mathrm{m}}_\infty}{\sigma_0}\right) = \left(\frac{E_{\mathrm{m}}}{V_{\mathrm{m}} E_{\mathrm{c}}}\right)^{1/2} \left(\frac{a}{a_0}\right)^{-1/2} \tag{3.5}$$

With $V_{\mathrm{m}} = 1$ (hence $E_{\mathrm{c}} = E_{\mathrm{m}}$) this represents the curve for the unreinforced matrix. The curve for a matrix without fibres is shown in figure 13. As an illustration, for 7 μm diameter carbon fibres of modulus 234 GPa in a glass with $K^{\mathrm{m}}_{\mathrm{Ic}} = 2$ MPa $\mathrm{m}^{1/2}$ and $E_{\mathrm{m}} = 58$ GPa, the modulus of the composite, at a volume fraction of 40% fibre is 128 GPa. Values of a_0 and of σ_0 depend on the assumed value of the interphase shear stress τ. If τ is taken as 10 MPa, $\sigma_0 = 535$ MPa and $a_0 = 6$ μm; for $\tau = 60$ MPa, $\sigma_0 = 968$ MPa and $a_0 = 1.8$ μm. Hence if the glass possessed flaws of length $(2a)$ of 30 μm, this would correspond to $a = 8.3a_0$ in the latter case and $2.5a_0$ in the former, giving cracking stresses for the material containing fibre, of *ca.* 750 MPa for $a_0 = 6$ mm ($\tau = 10$ MPa) and of *ca.* 1300 MPa for $a_0 = 1.8$ μm ($\tau = 60$ MPa). For the material without fibres the stress for cracking corresponds to complete fracture and is *ca.* 300 MPa from (3.4). Thus the effect of the fibres is most marked if the matrix contains long cracks so that $a \gg a_0$. A small value of a_0 corresponds to a large value of τ.

The experimental validation of this limit, given by

$$\sigma^{\mathrm{c}}_\infty / \sigma_0 = 1.331 \tag{3.6}$$

is very important for the use of reinforced ceramics. A really satisfying experimental proof for a fibre reinforced ceramic has not yet been given so far as I am aware. Evans & Zok's review states the result but gives no experimental proof. In some cases small matrix cracks may form at a stress below that corresponding to $\sigma^{\mathrm{c}}_\infty/\sigma_0 \approx 1.33$ (Kim & Pagano 1991). Such probably arise in regions starved of fibre or from a processing flaw.

4. Encouraging cracking

An aspect of the beneficial control of cracks is the use of composite materials to provide crashworthiness so as to save life under impact conditions in helicopters

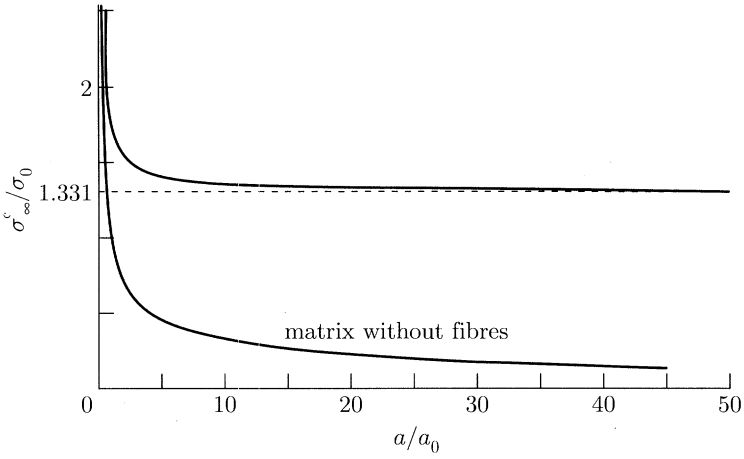

Figure 13. The critical stress on a composite for matrix cracking σ^c_∞ as a function of length $(2a)$ of the pre-existing crack in the matrix. $\sigma_0 = (\lambda K_{Ic}/\pi)^{2/3}$; $a_0 = (\sqrt{\pi}\, K_{Ic}/\lambda^2)^{2/3}$; $\sigma_0\sqrt{(\pi a_0)} = K_{Ic}$; $K_{Ic} = (V_m E_c/E_m)^{1/2} K^m_{Ic}$; $\lambda = (2V_f/V_m)[(2\pi\tau/r)(E_f E_c/E^2_m)]^{1/2}$; from Kelly (1987).

where it is used and in automobiles where it may be used. These ideas have been pioneered by Thornton and his co-workers (Thornton 1979) and Hull and his group (e.g. Hull 1991).

Fibre composite materials at their best are capable of absorbing more energy per unit *mass* than other materials. Values of the energy absorbed in grp tubes (vinyl ester matrix) can be as large as 160 MJ m^{-3} or some 70 kJ kg^{-1}. For instance, the energy dissipated per unit volume by composite rods with 50 vol.% aligned fibres crushed along the fibre axis increases almost linearly with fibre content and also almost linearly with increase in matrix yield strength. A small increase in energy absorption with increase in fibre diameter is also found. In metals, of course, and to some extent in thermoplastic materials, energy absorption in crushing is achieved by plastic deformation. In glass and in carbon reinforced epoxies and polyesters energy is absorbed by multiple microfracture processes. These processes are much more efficient in absorbing energy than those occurring in metallic structures. Furthermore the rate of crushing can be controlled and the initiation of crushing, so as to give the designer some freedom (Sigalas *et al.* 1991).

To give an example. If a square ended tube loaded in compression fails, it does so by one of three mechanisms: (i) Euler buckling, (ii) buckling leading to formation of a hinge and progressive folding, or (iii) by brittle fracture. Euler buckling may be avoided by proper choice of dimensions for a given elastic modulus. Catastrophic brittle failure is to be avoided since it is of no value as a means of energy absorption. Progressive folding and progressive crushing can both absorb very large amounts of energy. Progressive folding is found in thin walled tubes of continuous carbon and glass fibre (Thornton & Edwards 1982) and in tubes containing Kevlar (Farley 1986). It resembles closely what occurs under similar conditions with metal tubes of considerable ductility, and is favoured by matrix plasticity and flexible arrangements of fibres as would be expected.

What would not have been expected is that larger amounts of energy can be dissipated by controlling the progressive crushing of a completely brittle system. Progressive crushing is initiated by triggering fracture at a tube end, usually by bevelling the end, at a stress somewhat below the critical brittle fracture stress. A stable

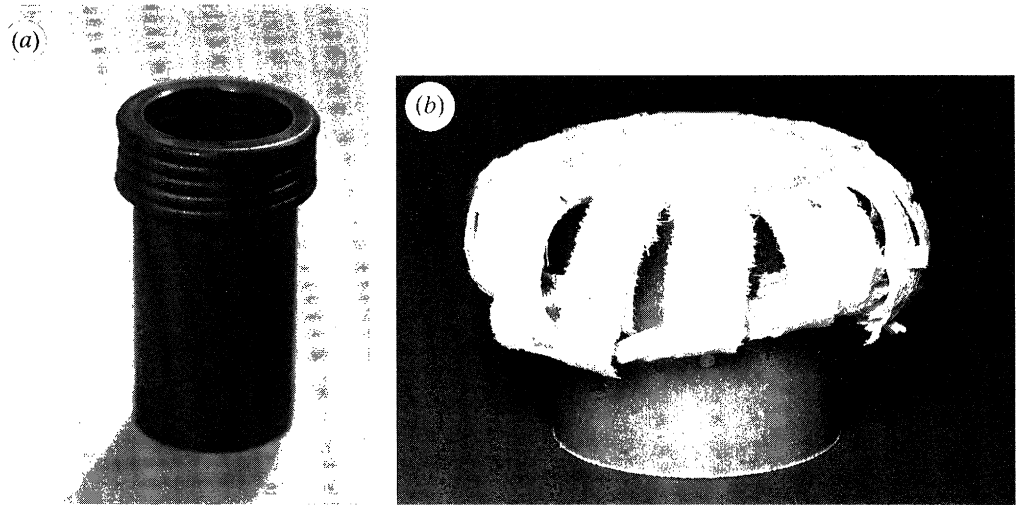

Figure 14. A comparison of crushed tubes of steel (*a*) and of woven glass cloth in epoxy resin (*b*) with $V_f \approx 0.54$. The tubes are each of 50 mm diameter and of about 2.5 mm wall thickness. Each was crushed at aboout the same speed. Photograph courtesy D. Hull.

zone of microfracture then progresses down the tube. Workers in the field distinguish two extreme modes of cracking designated as splaying or as fragmentation.

There is no great dependence on the process of fibre matrix debonding and related to this little dependence on the type of size applied to fibres. The energy of cracking also depends on the velocity of cracking, the variation with rate of cracking appears to be controlled essentially by the dependence of the matrix compressive stress on strain rate; being higher for higher strain rates. This is a beneficial effect; a higher impact velocity giving higher energy absorption.

Some values for the energy absorbed by different materials are combined in table 1. Figure 14 compares the failure of a steel tube with one made of a composite material. Of the total energy about one third is dissipated immediately as heat and of the remaining two thirds about half is due to the surface energy of the cracks. Composite tubes give very high values per unit of weight and values per unit of volume nearly as high as that of steel.

The composite also gives great flexibility to the designer. Progressive crushing by fragmentation or by splaying is related to the different micromechanisms of fracture in the composite material. By altering the distribution of fibres it is possible to change the micromechanisms of crush and hence to control the load bearing capacity of the tube via the specific crushing stress. By controlling the amount of fibres in the hoop direction, variation can be achieved between the two extremes of splaying (more hoop fibres, less splaying) and crushing.

The initiation of crushing can be controlled by the various trigger mechanisms (trigger mechanisms are also used with metal tubes) and another variable available to the designer is to choose the shape of the tube section besides variation in wall thickness. Friction between the platens and the tube material can also be varied depending on fibre content and type and on resin type. The geometrical variables are, of course, also available when designing with a single material, e.g. mild steel or PVC, but it is quite clear that here the composite offers much greater flexibility and provides much higher values per unit weight than do single-phase materials.

PHILOSOPHICAL TRANSACTIONS OF THE ROYAL SOCIETY A MATHEMATICAL, PHYSICAL & ENGINEERING SCIENCES

Table 1. *Energy absorbed in crushing tubes of various materials*

material	speed ($mm\ s^{-1}$)	specific energy ($J\ g^{-1}$)	($J\ ml^{-1}$)	density ($Mg\ m^{-3}$)
polycarbonate	4000	15	24	1.2
PVC	4000	brittle	—	1.4
mild steel	4000	25	195	7.8
aluminium	—	16	43	2.7
composite 0/90 – glass polyester	4000	55	104	1.9
SMC	4000	37	67	1.8?
glass-vinyl Ester. Eng. for maximum	—	70	133	1.9
carbon-epoxy	2000	110	176	1.6

5. Design of a high temperature resistant material

It is the use of cracks to inject a form of ductility into a completely brittle material that gives rise to the interest in the possibility of the use of ceramics as structural elements at very high temperatures. The idea being that if a very strong stable fibre were available it could be used when surrounded by a matrix to be load bearing and if the composite were overloaded then the rising stress–strain behaviour shown in figure 8, cf. also figure 11, would provide benign and safe failure. The temperatures in question to be of interest to, say, designers of high specific thrust turbine engines are 1500 °C and above, because ceramic materials with their generally low thermal conductivity cannot be cooled. That assumption of low thermal conductivity interestingly enough, is also called in question by the use of composites since composites can provide higher thermal conductivity than metals such as nickel, e.g. SiC/BeO. Carbon fibres would meet many of the requirements but burn in air at temperatures greater than 600 °C. However, I have argued (Kelly 1991) that their microstructure indicates the internal structure of the fibre which will be necessary for very high temperature service.

The chemical composition of the required material is very likely to be oxide. There is rather general agreement on this throughout the world (see, for example, Hillig 1993) and it arises because all the refractory metals oxidize rapidly at the temperature in question and materials such as silicon carbide and silicon nitride derive their oxidation resistance from the formation of a film of silica (SiO_2). This film is permeable so that oxygen diffusion occurs at a sufficiently rapid rate at temperatures greater than 1200 °C, to lead to oxidation of the silicon carbide or nitride. Silicon nitride, in common with other high melting point nitrides possesses a high vapour pressure and so tends to be volatile; an excellent review has been given by Raj (1993).

The required structure of the oxide fibre may be predicted from modern materials science and I would like to sketch the argument. We are aiming to design a material which will be practically useful and so a number of possibly interlinked properties are required. The material must be strong, stiff, resistant to oxidation, of a diameter to be weavable, and must be capable of withstanding thermal and cyclic stress fatigue

PHILOSOPHICAL TRANSACTIONS OF THE ROYAL SOCIETY A MATHEMATICAL, PHYSICAL & ENGINEERING SCIENCES

Table 2. *Target properties*

$\rho \leqslant 6$ Mg m^{-3} $\quad E$/s.g. $\geqslant 30$ GPa at 1500 °C, i.e. $E \geqslant 150$ GPa at 1500 °C
$\sigma \geqslant 0.5$ GPa at 1500 °C for $\geqslant 1000$ h in oxidizing atmosphere and $\epsilon \leqslant 0.5\%$ in that time
able to withstand oscillating stress and repeated thermal cycling
adequate fracture toughness, and benign, not sudden failure mode

besides being resistant to creep – say not extending by more than 0.5% in 1000 h – a set of formal requirements are shown in table 2.

There is also general agreement that the form of the fibre should be such that there are no transverse grain boundaries; whether that implies that it must be a single crystal is for discussion. A structure of equiaxed grains will not do.

Dislocations become mobile in pure single crystals of strong solids at temperatures greater than $0.5T_{\mathrm{m}}$, where T_{m} is the melting or the decomposition temperature. There is only one oxide with melting temperatures greater than 3200 °C and that is thoria. Some oxides with melting temperatures greater than 2500 °C are given in table 3. We thus must expect both single crystals and polycrystalline forms of the candidate material to exhibit creep. In single crystals glide and climb will be the only mechanisms of creep; except when surface diffusion plays a part, i.e. at temperatures greater than $0.85T_{\mathrm{m}}$. In polycrystals creep is far more complicated.

(*a*) *Creep of polycrystals*

When considering creep under a tensile stress due to the large number of mechanisms, all involving some kind of activated flow based on diffusion either of atoms or of point defects, a formula for the rate of creep emerges of the form

$$\dot{\epsilon} = \frac{AGb}{kT}\left(\frac{b}{d}\right)^{p}\left(\frac{\sigma}{G}\right)^{n} D_0 \exp\left(-\frac{Q}{kT}\right), \tag{5.1}$$

where G is shear modulus, b the Burgers vector, kT has its usual meaning. A, p and n are dimensionless constants. D_0 is the pre-exponential constant in the diffusion coefficient which exhibits exponential temperature dependence via the activation energy, Q, for the diffusion process. Cannon & Langdon (1983, 1988) list more than 20 mechanisms and give parameters Q, A and p in equation (5.1) for many materials. Both lattice mechanisms of creep and those based on intragranular motion of dislocations by glide or climb are considered; they are usually distinguished by $p = 0$ and $3 < n < 5$. Boundary mechanisms play a larger role in the creep of ceramics than in metals.

The most important parameter in determining long time resistance to creep is the parameter Q in equation (5.1). Scanning Cannon & Langdon's list for values of Q greater than, say, 500 kJ mol^{-1} (5 eV atom^{-1})†, one finds very few materials, namely Al_2O_3, $Al_2O_3SiO_2$, Al_2O_3MgO, MgO(?), $CaMgSiO_4$, PuO_2 and $SrZrO_3$ among the oxides together with SiAlON, NbC, SiC, TiC, ZrC, NbC and graphite among the carbides and Si_3N_4. As Cannon & Langdon point out there is a tendency to overstimate Q, particularly if n in equation (5.1) is large; to obtain an accurate value from an equation such as (5.1) a plot of $\ln(\dot{\epsilon}G^{n-1}T)$ against $(1/T)$ should be carried out.

† I choose this value because for smaller values of the activation energy rapid diffusion will occur at 1500 °C (see Kelly 1991).

PHILOSOPHICAL TRANSACTIONS OF THE ROYAL SOCIETY A MATHEMATICAL, PHYSICAL & ENGINEERING SCIENCES

Table 3. *Data on some high melting point oxides*

oxide	structure	MP @ ~ 0 °C	Young's modulus (RT) GPa	density (Mg m^{-3})
ThO_2	F	3200	250	9.86
UO_2	F	2800	240	10.9
MgO	H	2800	294	3.6
HfO_2	F	2700	210	9.7
ZrO_2	F (hiT)	2700	200	5.9
ss of ZrO_2 and rare earths ZrO_2 $0.15Y_2O_3$		2700		
CaO	H	2600	220	3.3
$SrOZrO_2$	P	2550		
BeO	W	2550	400	3.0
SrO	H	2500		4.7
Y_2O_3	F-def	2400		5.0
$MgOCr_2O_3$	S	2400		
$CaOZrO_2$	P	2350		
Cr_2O_3	as Al_2O_3	2250	320	5.2
$MgOAl_2O_3$	S	2100		
Al_2O_3		2000	400	4
$3Al_2O_32SiO_2$ mullite		1850	220	3.1

H, Halite; F, fluorite; W, wurtzite; S, spinel; P, perovskite.

Even with values of Q greater than 500kJ mol^{-1} appreciable creep rates will be found, larger than our target value and for this reason I do not believe that polycrystals can provide a material able to meet the arbitrary target set in table 2 with one important proviso as follows.

Grain boundary sliding and the emission and absorption of vacancies (or interstitial atoms) at a crystal boundary are aided by a component of the applied stress normal to the boundary or a shear stress parallel to the boundary. If the geometry of the grain structure is such that grain boundaries are all parallel or very nearly parallel to the applied stress, such phenomena are not aided. Under these conditions all grain boundary effects are greatly reduced (Versnyder & Shank 1970). The required microstructure is that sketched in figure 15. To ensure resistance to creep and to crack formation at grain boundaries transverse sections in a grain boundary otherwise parallel to the stress axis must be rigorously avoided.

If an oxide is available with the elongated fibrous microstructure we need to consider the scale of the lateral dimensions and whether or not a single crystal will be the best from. We believe that it will be necessary to have a fibrous form so as to provide toughness. The fibre must then be in the range of diameters d, where

$$50\text{ nm to }1\ \mu\text{m} < d < 5\ \mu\text{m to }10\ \mu\text{m}. \tag{5.2}$$

The upper limit being determined by the requirement of flexibility since the fibre will

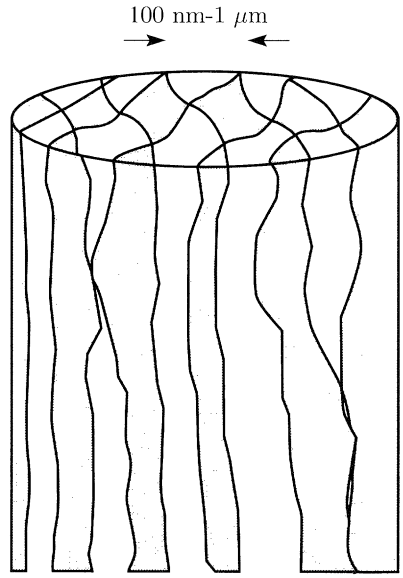

Figure 15. Schematic diagram of a microstructure in which transverse grain or phase boundaries are eliminated; see text.

need to be woven or possibly braided. The lower limit is set by the need to ensure handleability and to avoid a diameter range which can cause cancer in living beings.

Since the service temperature will be in excess of $0.5T_m$ dislocation motion must be expected to occur under stress. Cracks may also be formed adventitiously at the surface or due to impact or, if the slip systems exhibited do not show sufficient flexibility (in the form of a number of independent systems), then the dislocation motion itself may lead to internal cracks.

Whether dislocations will move at a stress of say 1 GPa at a temperature of 1500 °C depends upon the Peierls stress necessary to move the dislocations. From the evidence presented by other inherently strong solids, I do not believe the Peierls stress will be sufficiently high.

However, we should now examine how to design a material of very high Peierls stress. If the Peierls stress cannot be made sufficiently high to prevent some dislocation motion, then we must look for methods to restrict this. These must be, if possible, athermal methods of preventing dislocation motion, so that the barrier to dislocation motion cannot be overcome with the aid of thermal fluctuations.

(*b*) *Creep of single crystals*

Really quantitative estimates of the magnitude of the Peierls stress which could be used to identify those oxide crystals with very large yield stresses at large fractions of the melting temperature, with one possible exception (Gilman 1975), do not exist. Gilman's ideas do not appear to apply to materials with adequate oxidation resistance for our present purpose.

The atomic architecture of many oxides can be viewed as essentially close packed arrays of oxygen ions with cations located in the interstices. Since close packed arrangements are likely to show easier dislocation motion we do not expect those with the simpler crystal structures to show high creep resistance; the higher melting point oxides listed in table 3 all have simple structures of the halite or fluorite type.

PHILOSOPHICAL TRANSACTIONS OF THE ROYAL SOCIETY A MATHEMATICAL, PHYSICAL & ENGINEERING SCIENCES

In halite (NaCl) shown by the alkaline earth oxides, all the octahedral interstices in the close packed array of oxygens are filled but in zinc blende only one half of these contain cations. If slip takes place by the expected unit, then a change in local atomic environment ensues. The positions of the cations in those oxides possessing spinel structure ($MgO.Al_2O_3$) and in those with the perovskite structure (e.g. $SrO.TiO_2$ at room temperature) are then less symmetric. In the former the divalent cation occupies one eighth of the tetrahedral interstices and the aluminium one half of the octahedral interstices; the structure is cubic. The latter can be described as the oxygen plus divalent cation forming together a face-centred cubic structure with the tetravalent cation in the octahedral voids with only one quarter being filled. In fact in the perovskite structure speaking strictly, the coordination number of oxygen is only 2. The bonding is clearly directional and this is borne out by the fact that many of the perovskites are not cubic. Such a structure is expected to be quite resistant to slip. This would be expected to be greater in the garnets of which the composition could be written empirically as $3MnO.Al_2O_3.3SiO_2$ for the archetype.

Sometimes there may be only two cations eg in yttrium iron garnet. Another well-known synthetic garnet is YAG($3Y_2O_3.5Al_2O_3$) often used in solid state lasers. Writing the composition in this way while revealing the composition in an easy to remember form, obscures the fact that it is possible to substitute certain trivalent ions such as Y and Gd in the archetype structure for divalent manganese and tetravalent silicon. Silicon can be eliminated in synthetic garnets which gives rise to a whole series of microwave ferrites, etc. This illustrates the great fecundity and possibility of the oxides since so many substitutions are possible among the cations. Unfortunately for our purpose, few artificial garnets have high melting temperatures, and so none appears in table 3. Because ferrites possess the spinel or perovskite structures these have been much researched for their electric and magnetic properties. (J. H. Van Vleck drew an analogy between YAG for magneticians and drosophila (fruit fly) for geneticists!) It would be nice to see them researched for their high temperature mechanical properties.

If we are to find materials of high resistance to creep we must look for complex oxides with large shear moduli (the ideal shear strength (Kelly & Macmillan 1986) is proportional to this) and large Burgers vectors. We should also look for significant evidence of directional binding. Such is expected to be provided by cations of high charge and small radius. The directionality must not be too strong, however, or the structure may become too 'molecular'. Hillig (1993) has introduced a methodology for estimating the mechanical properties of oxides at high temperatures and has introduced a quantity called the apparent atomic volume of oxygen which serves as a measure of the mean interionic attraction. It is calculated from a knowledge of the crystal structure and of the cationic volumes in the structure, assuming that the radius of the O^{-2} ion is 1.26 Å, i.e. appropriate to sixfold coordination. The ions yielding small values of V_0 are taken to be attractive; they are Be, Al, and titanium plus possibly Cr. In summary the oxides which appear to have the greatest potential for providing creep resistance at high temperatures are, apart from the obvious criterion of a high melting point, those containing Be,Al,Ti,Cr with the most irregular and complicated crystal structures.

These ideas are to some extent borne out by the results of Deng & Warren (1995), who have estimated the creep strength of a variety of oxides by using the Larson Miller technique. The creep strength is defined as that tensile stress to produce a creep rate of 10^{-9} s^{-1} at 1600 °C. These are shown in figure 16 and table 3 shows some of the crystal structures and melting points. I have marked on the figure the fraction

PHILOSOPHICAL TRANSACTIONS OF THE ROYAL SOCIETY A MATHEMATICAL, PHYSICAL & ENGINEERING SCIENCES

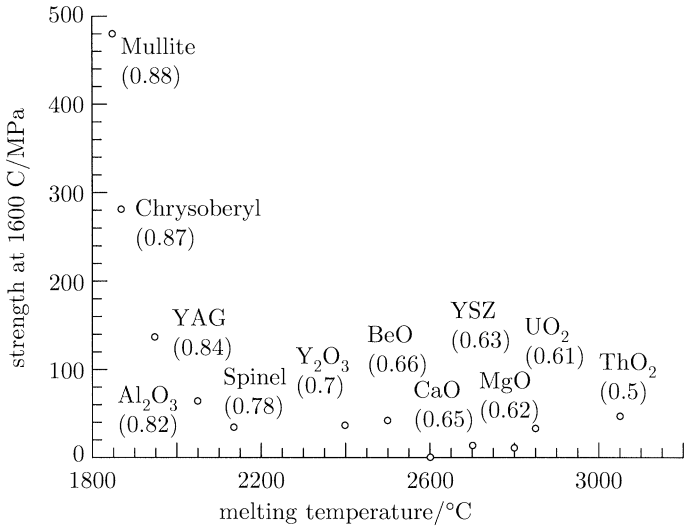

Figure 16. The creep strength at 1600 °C, defined as the stress to produce a creep rate of 10^{-9} s^{-1}, against melting temperature for several oxides.

of the melting point that 1600 °C represents. The agreement with the above ideas is really rather good. For instance, calcia and magnesia with the simplest (halite) crystal structure and uniform arrangement of the cations show least creep resistance despite magnesia's very high melting point. Thoria and urania, in which the oxygen anions are not close packed – in the fluorite structure the arrangement of fluorine ions is simple cubic – show somewhat higher resistance and thoria is a little stronger than urania because of the higher melting point. In beryllia and alumina only the basal plane of oxygen anions is a true plane; other anion containing planes are puckered. In addition, anionic and cationic movements differ in normal slip so these materials are more resistant than CaO and MgO and at similar homologous temperatures would do better than urania and thoria. The outstanding creep resistance is shown by mullite, chrysoberyl and yttrium aluminium garnet with their complicated crystal structures, mullite showing a creep strength of nearly 500 MPa at close to 0.9 of the melting point. The possible exception to this agreement is spinel $MgO.0.9Al_2O_3$. However, the magnesia spinel is likely to be less resistant to creep than other spinels, e.g. $MgO.Cr_2O_3$ (see earlier discussion of Hillig's criterion), which also has a higher melting point than $MgO.Al_2O_3$.

(*c*) *Restricting dislocation multiplication*

However, a material of high Peierls stress may not be enough. If the yield stress is locally exceeded dislocations may be produced. Secondly, we may not wish to restrict the chemical composition to those materials with a very high Peierls stress. It may be that sufficiently oxidation resistant materials with high Peierls stresses are not suitable because of other properties, e.g. high CTE. We therefore look for methods of strengthening which could be applied at high temperatures even to materials of low Peierls stress. A third reason is that cracks may be introduced and we wish to stop these expanding. The analogy between a crack and a dislocation pointed out in § 2 *b*, *c* suggests that if we can stop dislocations from expanding we will also hinder crack growth.

We therefore look for methods of preventing dislocation multiplication and because

the methods must operate effectively at very high fractions of the melting point of the host material, we must have recourse to strengthening methods which are athermal, that is to say, barriers to dislocations that may not be overcome with the aid of thermal fluctuations at temperatures less than the melting temperature. There are two: (i) opposing dislocation motion by change of elastic constant, and (ii) by change of lattice parameter.

These are the two parameters to consider, since we know that crystalline solids melt by a type of order–disorder reaction, and possess a crystal lattice and a measurable rigidity within a few degrees, if not at, their melting points.

(i) *Difference of elastic constant*

Dislocation sources may be prevented from operating by making use of the facts that the line energy of a dislocation depends on the square of the Burgers vector and on the value of the elastic shear modulus. We deal first with the latter.

Straight dislocations moving in a medium of elastic shear modulus G_{A} will not move into a material of higher elastic shear modulus G_{B} unless a stress,

$$\sigma_{\mathrm{a}}^{\mathrm{A}} \geqslant \sigma_{\mathrm{i}}^{\mathrm{A}} + \sigma_{\mathrm{m}}, \tag{5.3}$$

is exceeded (Koehler 1970; Lehockzky 1978*a*, *b*). Here $\sigma_{\mathrm{i}}^{\mathrm{A}}$ is the (tensile) stress required to move a single dislocation in a large specimen of the material; the friction stress, which we will identify with the Peierls stress. σ_{m} is given by

$$\sigma_{\mathrm{m}} = \left(\frac{G_{\mathrm{B}} - G_{\mathrm{A}}}{G_{\mathrm{B}} + G_{\mathrm{A}}}\right)\frac{G_{\mathrm{A}}}{8\pi}. \tag{5.4}$$

The geometry considered by Lehoczky and Koehler is that of a straight dislocation in material A being forced against a plane boundary between layers of the two materials. If t_{A} is the thickness of the layer of material A the operation of a Frank–Read source within A requires a tensile stress applied to A of approximately

$$\sigma_{\mathrm{a}}^{\mathrm{A}} \geqslant \sigma_{\mathrm{i}}^{\mathrm{A}} + \frac{2\alpha G_{\mathrm{A}} b_{\mathrm{A}}}{t_{\mathrm{A}}/2}. \tag{5.5}$$

Operation of a Frank–Read source in material A then requires that the applied stress given by equation (5.5) be less than that given by equation (5.3) which for thick layers (large t_{A}) will always be the case. However, if layers of A are made sufficiently thin such that the second term in equation (5.5) exceeds the value of σ_{m} in equation (5.4) then Frank–Read sources cannot operate within material A.

The thickness of the foil necessary to suppress the operation of Frank–Read sources is thus given by

$$t_{\mathrm{crit}} \leqslant \left(\frac{G_{\mathrm{B}} - G_{\mathrm{A}}}{G_{\mathrm{B}} + G_{\mathrm{A}}}\right) 32\pi\alpha b_{\mathrm{A}} \tag{5.6}$$

and for thickness less than this, single dislocations only will move within material A. The stress to move single straight dislocations within material B will be given by $\sigma_{\mathrm{i}}^{\mathrm{B}}$ and if this is exceeded than dislocations may multiply within B so long as the thickness of the material B is sufficiently large. If the layers of material B were also small then again only single dislocations could move. The conclusion is that provided a layered composite material were made with thickness of the component layers less than that given by (5.5), then dislocation multiplication could not occur unless a

PHILOSOPHICAL TRANSACTIONS OF THE ROYAL SOCIETY A MATHEMATICAL, PHYSICAL & ENGINEERING SCIENCES

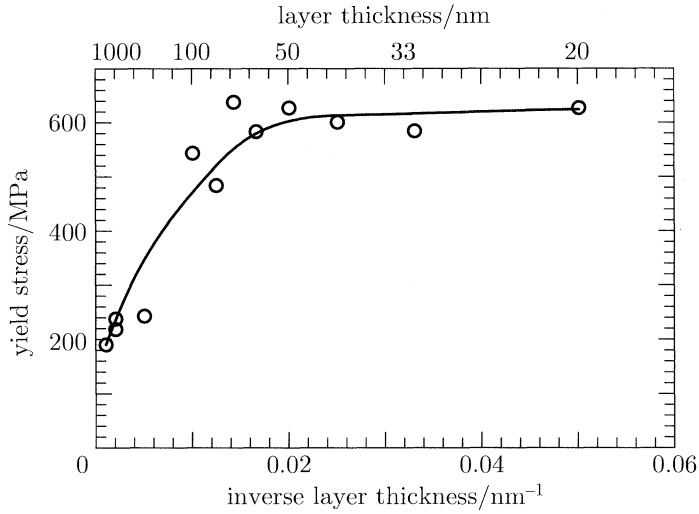

Figure 17. A plot of yield stress at room temperature versus layer thickness for layers of equal thickness of pure aluminium and copper. Replotted from data given in Lehoczky (1978).

stress given by

$$\sigma_{\mathrm{a}} \geqslant \sigma_{\mathrm{i}}^{\mathrm{A}} + \left(\frac{G_{\mathrm{B}} - G_{\mathrm{A}}}{G_{\mathrm{B}} + G_{\mathrm{A}}}\right)\frac{G_{\mathrm{A}}}{8\pi} \tag{5.7}$$

is exceeded.

These ideas have been verified for thin foils of pure metals where remarkably high strengths are obtained if thin layers are properly made (Lehoczky 1978*a*, *b*). A replot of Lehoczky's results is shown in figure 17. I suggest that the same ideas may be applied to ceramic crystals which was also suggested by Koehler, at least for ionic crystals.

If thin individual monocrystals with differing elastic constants are placed side by side extensive glide will not be possible unless an external stress is applied which exceeds that given by equation (5.7). Lehoczky and Koehler give formulae that apply to thin foils of dissimilar materials in contact. They also assume, as was apparently the case in Lehoczky's experiments, that the boundaries between the metals do not provide sources of dislocations. The slip systems available in ceramic materials are much more restricted than in FCC metals so I believe that provided dissimilar ceramic materials were in intimate contact Lehoczky and Koehler's formulae would apply also to thin foils of these. I see no reason for not extending the idea in two ways, namely to apply it to small crystals of size less than t_{crit} of two dissimilar materials in contact even if these are not foil shaped. Secondly to assume that the same idea applies to differently oriented grains of the same material.

It is proposed therefore that one microstructure most resistant to dislocation glide at high temperatures will consist of columnar grains of either the same or of dissimilar material, the individual grains being of lateral dimension less than t_{crit}. Under these conditions plastic flow by the motion of dislocations should not occur at a stress less than that given by equation (5.7). If dislocation multiplication is prevented for gliding dislocations it will also be prevented for multiplication by climb; if all multiplication is prevented I am assuming that creep deformation will be strongly opposed.

(ii) *Difference of lattice parameter*

Again we consider parallel layers in this case with a coherent interface and initially with identical elastic constants. If the layers are of thickness d and the Burgers vectors of the dislocations in the two materials are b_A and b_B the misfit strain is $(b_A - b_B)/b_A = \epsilon_0$. We assume that the misfit strain is small, say up to a few percent.

If a dislocation passes say from material A into material B a dislocation of magnitude $b_A - b_B$ will be left at the interface (see Friedel 1964). Suppose that b_A and b_B are parallel to one another. The force per unit length F between the misfit dislocation and the dislocation of Burgers vector b_B will be

$$F = \frac{G|b_A - b_B|b_B}{2\pi r} \tag{5.8}$$

when the two dislocations are at a distance r apart.

The maximum force will occur when $r \approx b$, the inner cut-off radius, giving

$$F_{max} = G\Delta b/2\pi, \tag{5.9}$$

writing $\Delta b = (b_A - b_B)$.

To drive a dislocation across the interface requires, therefore a shear stress (τ) in the glide plane and in the glide direction of

$$\tau b = G\Delta b/2\pi, \quad \text{or} \quad \tau \approx G\epsilon_0/2\pi. \tag{5.10}$$

To operate a Frank–Read source in either layer will require an applied stress within that layer which produces a shear stress of at least

$$\tau = Gb/d \tag{5.11}$$

(e.g. Hirth & Lothe 1968).

Equating these two values we have

$$G\epsilon_0/2\pi = Gb/d, \quad \text{or} \quad \epsilon_0 d = 2\pi b \tag{5.12}$$

as the minimum thickness of layer within which a Frank–Read source can operate.

The thickness d may be equated with the thickness at which an epitaxial layer of strain (misfit) can relax by the operation of a Frank–Read spiral or planar source. Beanland (1992) gives a much more sophisticated derivation of equation (5.12). The thickness d_r calculated as above is larger by the factor 2 than the critical thickness (d_c) obtained by equating the strain energy of the layer before and after relaxation with that for the formation of a layer of misfit dislocations (Matthews & Blakeslee 1974). Experiment shows that layers, particularly of semiconductor materials do not in fact relax until a thickness several times that given by Matthews & Blakeslee's criterion, which is given by the product $d_c\epsilon_0 = b$.

For example, GaAs and related compounds are brittle at room temperature while at 400 °C it can be deformed plastically under a small stress; 400 °C is $0.44T_m$. It is well established that thin, defect free epitaxial layers of, for example, $In_xGa_{1-x}As$ can be grown with elastic coherency strains of up to a few percent at temperatures of 600 °C ($0.57T_m$) and such layers have been annealed at temperatures of 1050 °C without relaxation taking place ($0.87T_m$) (see Gillin *et al.* 1993).

Since elastic strains in excess of 1% can be supported by a single thin layer, at temperatures close to the melting point, it is natural to suggest that this non-thermal strengthening can be made to operate in a multilayer composite structure of materials of very high melting points. That such multilayer structures can be manufactured with high melting point oxides is not in doubt (e.g. Revcoleschi & Dhalenne 1993).

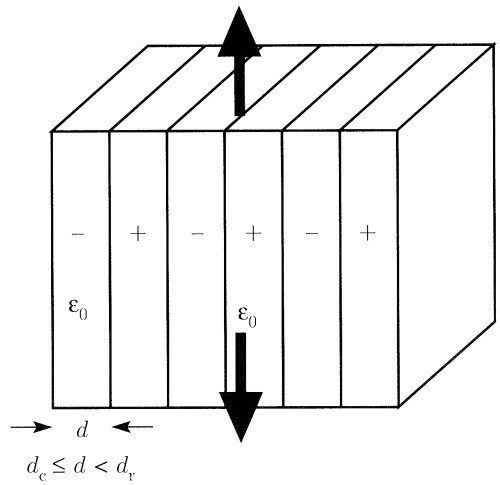

Figure 18. Schematic diagram of a layered structure consisting of epitaxial layers strained alternatively positively and negatively with respect to one another. The arrows represent the applied stress.

The type of microstructure envisaged is shown in figure 18. The layers are supposed to be of the same width and elastic modulus. There will be zero nett strain in the specimen, with alternate layers strained positively and negatively as indicated, with each layer of thickness certainly less than d_r and possibly as thin as d_c. It should be borne in mind that the relaxation thickness d_c is independent of the elastic properties of the material.

If our target is a sustainable stress of 1 GPa and the elastic modulus of the layers is 200 GPa then we need a nett strain of ϵ_n of 0.5% without generation of dislocations occurring. This should be achievable provided layers are made of thickness $d_c = b/2\epsilon_n$ of some $100b$. The factor of 2 occurring because it must be remembered that in the configuration shown in figure 18, the layers in tension will be sustaining a strain of $(\epsilon_n + \epsilon_0)$ when an additional strain of ϵ_n is imposed upon the composite. It may be possible to use layers of thickness between d_c and d_r depending on the value required for the strength of the composite. A large value of b the Burgers vector of the misfit dislocation will be an advantage.

Hafnia (MP 2700C, structure fluorite) and Zirconia (MP2700C, structure fluorite at high temperature or stabilized) have lattice parameters differing by 1% (5.12 Å and 5.07 Å) respectively. Using Dunstan *et al.*'s (1991) criterion for the thicknesss d_c gives a value of $102b$ where $b = 5.07/\sqrt{2} = 3.58$ Å and so layers should remain coherent until a thickness of 36.5 nm. With $d_r = 2\pi d_c$ layers should remain coherent until a thickness of some 203 nm or about 0.2 μm. The attainable strength would be $0.005E_c$ or about 1 GPa taking E_c to be the elastic modulus of zirconia; following Hillig (1993) that of hafnia should be very similar.

The desired microstructure must be: (*a*) an aligned one, separating (preferably with a coherent interface) (*b*) materials possessing the highest possible Peierls stress, with (*c*) a change of lattice parametrer and a change of elastic modulus across the interface.

The chemical compositions should be as close as possible, if not identical, so as to avoid interdiffusion at high temperatures. Or, the two phases should be in thermodynamic equilibrium, e.g. a eutectic.

This argument shows that the scale of the microstructure should be of dimensions not greater than 1 μm and possibly no coarser than 100 nm.

(*d*) *Packing of the fibres*

Returning to figure 15 this is now to be regarded as representing the internal 'composite' structure of a fibre with the cross sectional diameter given by the inequality (5.2). Such fibres need to be brought together themselves into a composite. That is, they must be placed within a matrix, the interaction of fibre and matrix providing the overall toughness; see § 3.

The presence of a matrix of dissimilar chemical composition to that of the fibres raises the question of chemical compatibility at high temperatures. It is interesting to speculate how the amount of matrix necessary could be reduced to a minimum. To do this the fibrous arrangement must be able to resist a general deformation.

Parkhouse & Kelly (1996) have investigated repeating patterns of infinitely long straight bars to find out what is the tightest packing that can be devised for the cases of material being distributed equally in 3, 4 and 6 directions. The cross section of the bars is chosen to maximize the packing density. For three directions normal to the faces of a cube the fibre volume fraction V_f is 3/4. They discovered arrangements based on the regular tetrahedron and on the rhombic dodecahedron which follow the same 'rule' in that the directions of the bars are the same as the normal to the faces of their associated solids and their bar sections are the same as the faces of their associated solids. The values of V_f are 1/2 and 1/3 respectively. In both cases closer packing can be obtained if the cross sectional shape is changed. In the tetrahedral case a regular hexagon as cross section yields a value of V_f of as high as 3/4 and in the case of a rhombic dodecahedron choice of cross section of a truncated rhombus or irregular hexagon leads to a value of V_f as high as 5/8 (0.625). The results are collected in table 4, together with values of the elastic modulus assuming that the fibres are stretched only from their ends.

The arrangement of fibres along the normals to the faces of a rhombic dodecahedron provides fibres in six directions and ensures a non-zero elastic modulus in all directions. Whether an arrangement of fibres can provide an elastically isotropic composite is an intriguing question. Fibres must be arranged in at least six directions (because of the six independent components of the stress (or strain) tensor). A regular solid with face normals running in six directions in space, each equally disposed with respect to the other, is the regular dodecahedron. Christensen (1987) has proved that infinitely slender fibres arranged in this way with each fibre making an angle of $\arctan 2$ to the others provides an elastically isotropic arrangement but the specification of infinite slenderness implies an elastic modulus of zero. Kelly & Parkhouse have explored arrangements of bars with pentagonal cross sections each making an angle of $\arctan 2$ to every other. A small number pack tightly; the question is whether a periodic arrangement exists. An arrangement involving exact translational symmetry, as in the cases of the tetrahedral and rhombic dodecahedral packing, is not possible since it would require translational symmetry normal to a fivefold axis of rotational symmetry. However, an 'almost' periodic arrangement can repeat indefinitely – what is quite meant by 'almost' in this case is not precise – (Penrose 1974); one arrangement being discovered by Ogawa & Hizume (personal communication). For this particular case the volume fraction found, so far, by Parkhouse & Kelly yields a volume fraction of only 0.15(1/6). There is a possibility of a much larger density of packing so whether true isotropy can be obtained with fibres with a useful volume fraction is still an unsettled question.

PHILOSOPHICAL TRANSACTIONS OF THE ROYAL SOCIETY A MATHEMATICAL, PHYSICAL & ENGINEERING SCIENCES

Table 4. *Density of packing of long straight fibres*
(E_f is the modulus of the fibre; 'max' and 'min' are the extreme values of the array.)

fibre directions	fibre cross section	E_{max}	E_{min}	volume fraction
cube edge	square	$E_f/4$	0	0.75
tetrahedral	equi. triangle	$E_f/8$	0	0.5
tetrahedral	reg. hexagon	$3E_f/16$	0	0.75
normals to rhombic dodecahedron	35.3° rhombus	$E_f/15$	$E_f/27$	0.33
normals to rhombic dodecahedron	irregular hex. or trunc. rhombus	$E_f/8$	$5E_f/72$	0.625 (5/8)
regular dodecahedron	regular pentagon	$(E_f/6)$ V	$(E_f/6)$ V	$? > 0.15$

6. Monitoring of new materials: composites in particular

Because of the way in which composites are manufactured it is relatively easy (compared with other materials) to embed sensors and activators within them. This may give to the material the ability to adapt to changing environment (applied forces, change of chemical environment, ageing of the structure). An example of an adaptive feature is a composite containing optical fibres (perhaps in addition to the glass fibres of normal diameter which are used for reinforcement); shape memory alloy or piezoelectric actuators, which have the ability to sense a load, or to measure stiffness or damping. These actuators could also generate force so as to change (slightly) the shape of the composite and to dampen vibration of the structure. Optical fibres produced for long distance telecommunication (e.g. Midwinter 1984) are so important here because the methods developed to check them for defects in their manufacture can be turned to advantage so as to use them as very sensitive sensors with an ability, for instance, to locate a defect to within a few centimetres in 100 m of fibre. Their breaking strengths are investigated by using specimen lengths of greater than 1 km (e.g. Ritter & Jakus 1981). Rogers (1988) gives a comprehensive account of the physics of the operation of distributed optical fibre sensors.

One of the features that intrigues, particularly the civil engineering community and more particularly those concerned with structural safety, is the possibility of providing modern materials systems with a type of birth to retirement health policy. This would refer to the possibilty of using sensors to control the manufacturing process in which an engineering artefact is created so as to ensure not only quality but also to minimize waste and to achieve the goal of getting it 'right first time'. With the same network of sensors the 'health' of the system could be monitored throughout the life of the artefact; in principle the actuator system could be used to control structural damage and/or modify a structures' behaviour or performance so as to elude damage. The ageing process of the structure could also be monitored in order to determine when the artefact should be repaired or taken out of service (retired).

These promises are not yet realized. I believe that many of them will be. I will give some examples of what has been realized; this will indicate achievements and also the formidable difficulties.

PHILOSOPHICAL TRANSACTIONS OF THE ROYAL SOCIETY A MATHEMATICAL, PHYSICAL & ENGINEERING SCIENCES

An example of monitoring of fabrication is as follows. A fibre optic sensor consisting of a step (refractive) index fibre coated with polymide is placed within a carbon fibre reinforced PEEK laminate (APC-2 prepreg) and while the composite is heated to 390 °C and cooled under presssure the signal intensity variations of HeNe 633 nm radiation are monitored. A special coating on the optical fibre is necessary to match the temperatures encountered during cure. Crystallization of the matrix and the onset of thermal frozen in strain can be detected and in principle corrected for (Davidson *et al.* 1992).

In the monitoring of aircraft structures, fibres of the type used in optical communication systems (e.g. step-index multimode fibres) are now embedded within a structure during fabrication (e.g. Hofer 1987). The fibres are usually of larger diameter than the reinforcing fibres of glass, Kevlar or carbon, but it is established in several cases that their incorporation does not reduce the strength of the structure (e.g. Glossop *et al.* 1990; Roberts & Davidson 1991). Monitoring of this type is extremely important for planar composite structures because impact damage on cfrp is often not visible on the exterior surface which is the one impacted. This makes visual detection impossible.

Although some of the problems of multiplexing and interrogating a large number of fibres have been solved and damage such as delamination failure around bolt holes, groups of broken fibres and the growth of cracks have all been successfully detected, only the fracture of the sensing fibre and/or attenuation of the signal have (according to my knowledge) so far been used in practice. The full power of the technique has thus not yet been fully realized.

In principle, phase shift, back-scattered light, change of plane of polarization and the elasto-optic effect can all effect the intensity and so could be used to detect change of properties (which is related to damage) in a region near to an embedded optical fibre. Optical fibres may also be configured so as to contain an intracore grating, a fibre optic Bragg grating which, because of the extremely high sensitivity to change of wavelength, may be specifically designed to measure mechanical strain at particular points along a fibre. They have been successfully embedded in composites using continuous resin transfer moulding techniques (e.g. Friebele *et al.* 1994).

The use of fibres embedded within a composite to monitor structural changes can be described as *passive*; the material is perceptive of its condition. Active mechanical control may be exercised by embedding an element, say, a wire or fibre which can be commanded to change its shape by heating (shape memory alloys), or by applying an electric field (piezoelectric material). Examples of both of these methods appear in the literature (e.g. Rogers *et al.* (1988) and Rogers (1993), who is a leader in the field in the USA, and Davidson (1994), a European exponent; see also Roberts *et al.* (1994)).

The shape memory alloy (SMA) Nitanol (roughly 50:50 Nickel titanium) has a martensitic transformation near room temperature (*ca.* 50 °C) and this transformation is also thermoelastic. When plastically deformed, within the correct temperature range, the deformation occurs by means of the transformation and so if a fibre, for example, is stretched at a low temperature then on heating it may recover its length by as much as 10%. The elastic modulus of the alloy is some 60 GPa at high temperature and 28 GPa at the lower. The yield strength of the martensite is some 620 MPa at the higher temperature (see, for example, Perkins (1986) for a review).

Structural motion and shape control can then be achieved by embedding SMAs in the material off the neutral axis on both sides of a beam in agonist–antagonist pairs,

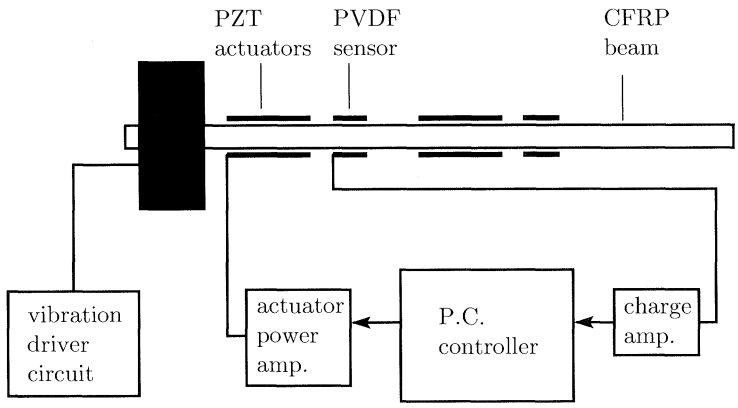

Figure 19. Schematic diagram of an active damping system; from Roberts *et al.* (1994).

as they are called, as in a human arm. Before embedding, the wires are 'plastically' prestrained and are constrained from contracting during the curing of the composite. These wires are actuators and an integral part of the structure. They may be triggered by resistance heating to cause a uniformly distributed shear load along the length of the wires (not just at the ends). This shear load can cause the structure to bend in a controlled manner.

Because the elastic modulus of the alloy is much higher at the elevated temperature and the yield strength also quite high, the wires which have been heated to cause bending to one side of the neutral axis may be allowed to cool and then plastically deformed again by heating the wires on the other side of the neutral axis so as to bend the beam in the opposite sense.

Despite this great versatility shown by SMAs their use must be limited to cases where low frequencies of vibration or oscillation are involved and where large forces are necessary. Roberts *et al.* (1994) describe a user friendly system for active structural damping which is illustrated in figure 19 and figure 20. While not strictly a composite system since the sensors and actuators are not of fibre form nor embedded within the composite, nevertheless, it illustrates well the principles.

Piezoelectric sensors made of PVDF measure the *strain* (not the deflection) through the change in polarization induced. PZT actuators are then used to reduce (or could enhance) the vibrations. The method is usually employed to monitor and to reduce unwanted oscillation. The manipulation of these materials – polymer sensors – high g_{31} coefficients and piezoelectric activators (high d_{31}) is not simple, e.g. PZT is 'carrot' brittle. The system can deal with many mode vibrations (many harmonics) which is important since so many uses are for damping of what are, in effect, single modes of vibration.

In the far future it is envisaged that the use of embedded sensors together with activators coupled with feed back between the two and a memory of past responses will lead to an 'intelligent material system' which (or should it be who?) not only knows how it feels, but is also able to do something about it should it feel unwell. All this from the discovery of how to make strong and stiff fibres and optical fibres; neither of which was known 34 years ago!

I am very grateful to many colleagues for help over the years, and in connection with this lecture, in particular, John Aveston and Neil McCartney of the NPL; Graham Parkhouse, Paul Smith, David Dunstan, and David Hannant of the University of Surrey; Roger Davidson from AEA and

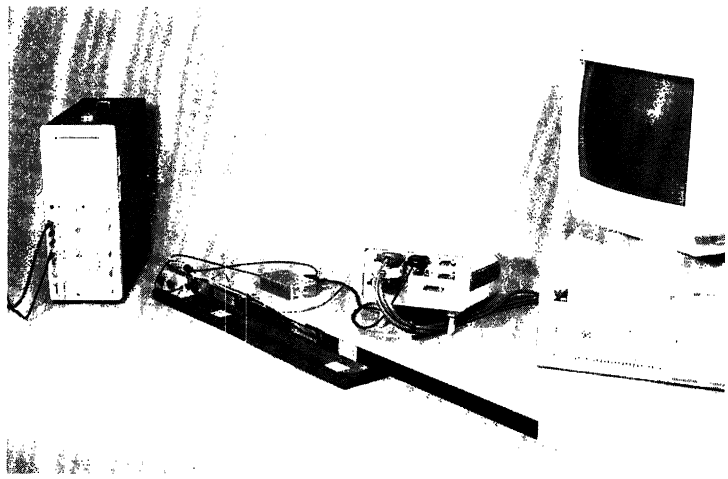

Figure 20. A photograph of the experimental set up shown schematically in figure 19; from Roberts *et al.* (1994).

Clive Phillips from Kobe Steel. I am also grateful to the following, who have helped me with the preparation of illustrations for this lecture: Malcolm McLean, Derek Hull, Carl Cady, (Tony Evans), Lalitesh Chandra, Bill Clyne, Mike Shaw, Scott Roberts, Eric Dore. Alan Cottrell first inspired me with this subject in 1960 for which I am continually grateful. I am also grateful to the Leverhume Trust for financial support, which enabled me to carry forward the material mentioned in § 5 *c*(ii) and § 5 *d*.

References

Abrate, S. 1991 Matrix cracking in laminated composites – a review. *Compos. Engng* **1**, 337–353.

Albers, W. 1986 Composite materials: non mechanical properties. In *Encyclopedia of materials science engineering* (ed. M. B. Bever), vol. 2, pp. 763–767. Pergamon Press.

Allen, D. M. 1994 *Damage evolution in laminates in damage mechanics of composite materials* (ed. R. Talreja), pp. 79–115. Elsevier Science.

Ashby, M. F. 1993 Criteria for selecting the components of composites. *Acta Metall. Mater.* **41**, 1313–1335.

Ashton, J. E., Halpin, J. C. & Pettit, P. H. 1969 *Primer on composite materials*. Stamford, CT: Technomic.

Aveston, J. A., Cooper, G. A. & Kelly, A. 1971 Single and multiple fracture. In *Int. Conf. Proc. National Physical Laboratory: The Properties of Fibre Composites*, pp. 15–26. Guildford: IPC Science and Technology.

Bailey, J. E., Curtis, P. T. & Parvizi, A. 1979 On transverse cracking and longitudinal splitting of glass and carbon reinforced epoxy cross ply laminates and the effect of Poisson and thermally generated strain. *Proc. R. Soc. Lond.* A **366**, 599–623.

Baldus, H. P. & Passing, G. 1994 Studies on SiBN(C)-ceramics: oxidation and crystallisation behaviour lead the way to applications. *Mater. Res. Soc. Symp. Proc.* **346**, 617–622.

Beanland, R. 1992 Multiplication of misfit dislocations in epitaxial layers. *J. Appl. Phys.* **72**, 4031–4035.

Birchall, J. D. 1983 Cement in the context of new materials for an energy-expensive future. *Phil. Trans. R. Soc. Lond.* A **310**, 31–42.

Cannon, W. R. & Langdon, T. G. 1983 Creep of ceramics. 1. Mechanical characteristics. *J. Mater. Sci.* **18**, 1–50.

Cannon, W. R. & Langdon, T. G. 1988 Creep of ceramics. 2. An examination of flow mechanisms. *J. Mater. Sci.* **23**, 1–20.

PHILOSOPHICAL TRANSACTIONS OF THE ROYAL SOCIETY A MATHEMATICAL, PHYSICAL & ENGINEERING SCIENCES

Christensen, R. M. 1987 Sufficient symmetry conditions for isotropy of the elastic moduli tensor. *Trans. ASME* **54**, 772–777.

Cooper, G. A. & Sillwood, J. M. 1972 Multiple fracture in a steel reinforced epoxy resin composite. *J. Mater. Sci.* **7**, 325–33.

Davidson, R. 1994 Smart composite materials systems. In *Concise encyclopedia of composite materials revised* (ed. A. Kelly), pp. 259–265. Pergamon Press.

Davidson, R., Roberts, A., Brabon, S. & Yates, T. 1993 Vibration reduction in composite structures. In *ECCM smart composites workshop* (ed. P. Gardiner, A. Kelly & A. R. Bunsell), pp. 89–94. Abington, Cambridge: Woodhead.

Davidson, R., Roberts, S. S. J. & Zahlan, N. 1992 Fabrication monitoring of APC-2 using embedded fibre optic sensors. *Proc. ECCM* (ed. A. R. Bunsell, J. F. Jamet & A. Massiah), vol. 5, pp. 441–446.

Deng, S. & Warren, R. 1995 Creep properties of single crystal oxides evaluated by a Larson–Miller procedure. *J. Eur. Ceram. Soc.* **15**, 513–520.

Dunstan, D. J., Young, S. & Dixon, R. H. 1991 Geometrical theory of critical thickness and relaxation in strained-layer growth. *J. Appl. Phys.* **70**, 3038–3044.

Evans, A. G. 1995 Ceramics and ceramic composites as high temperature structural materials: challenges and opportunities. *Phil. Trans. R. Soc. Lond* A **351**, 511–527.

Evans, A. G. & Zok, F. W. 1994 The physics and mechanics of fibre-reinforced brittle matrix composites. *J. Mater. Sci.* **29**, 3857–3896.

Evans, K. 1990 Tailoring the negative Poisson ratio. *Chemistry and Industry*, October, pp. 654–657.

Farley, G. L. 1986 Effect of specimen geometry on the energy absorption capability of composite materials. *J. Comp. Mater.* **20**, 390–400.

Friebele, E. J., Askins, C. G., Putnam, M. A., Florio Jr, J., Fosha Jr, A. A., Donti, R. P. & Mosley, C. D. 1994 Distributed strain sensing with fiber Bragg grating arrays embedded in CRTM composites. In *2nd European Conf. on Smart Structures and Materials* (ed. A. McDonach, P. T. Gardiner, R. S. McEwen & B. Culshaw). *Proc. SPIE*, pp. 338–341.

Friedel, J. 1956 *Les dislocations*, 1st edn. Paris: Gauthier-Villars.

Friedel, J. 1964 *Dislocations*. Reading, MA: Addison-Wesley.

Gillin, W. P., Dunstan, D. J., Homewood, K. P., Howard, L. K. & Sealy, B. J. 1993 Interdiffusion in In Ga As/Ga As quantum well structures as a function of depth. *J. Appl. Phys.* **73**, 3782.

Gilman, J. J. 1975 Flow of covalent solids at low temperatures. *J. Appl. Phys.* **46**, 5110–5113.

Glossop, N. D. W., Dubois, S., Tsaw, W., Leblanc, M., Lymer, J., Measures, R. M. & Tennyson, R. C. 1990 Optical fibre damage detection for an aircraft composite leading edge. *Composites* **21**, 71–80.

Hale, D. K. 1976 The physical properties of composite materials. *J. Mater. Sci.* **11**, 2105–2141.

Herakovich, C. T. 1984 Composite laminates with negative through-the-thickness poisson's ratios. *J. Comp. Mater.* **18**, 447–455.

Hillig, W. B. 1993 A methodology for estimating the mechanical properties of oxides at high temperatures. *J. Am. Ceram. Soc.* **76**, 129–138.

Hirth, J. P. & Lothe, J. 1968 *Theory of dislocations*. McGraw-Hill.

Hofer, B. 1987 Fibre optic damage detection in composite structures. *Composites* **18**, 309–316.

Hull, D. 1991 A unified approach to progressive cracking of fibre reinforced composite tubes. *Comp. Sci. Tech.* **40**, 377–421.

Kelly, A. 1987 Composites for the 1990s. *Phil. Trans. R. Soc. Lond.* A **322**, 409–423.

Kelly, A. 1990 Novel forming methods (for composites). New Materials and their applications. In *Proc. 2nd Int. Symp. on New Materials Inst. of Physics Conference Series no. 111* (ed. D. Holland), pp. 5–12.

Kelly, A. 1991 Design of a high temperature structural material. In *2nd Int. Conf. on Advance Materials and Technology* (New Compo '91 Hyogo, Japan), pp. 205–216.

Kelly, A. & Tyson, W. R. 1965 Tensile properties of fibre reinforced metals: copper/tungsten and copper/molybdenum. *J. Mech Phys. Solids* **13**, 329–350.

PHILOSOPHICAL TRANSACTIONS OF THE ROYAL SOCIETY A MATHEMATICAL, PHYSICAL & ENGINEERING SCIENCES

Kelly, A. & MacMillan, N. H. 1986 *Strong solids*, 3rd edn, p. 24. Oxford University Press.

Kendall, K. 1994 Adhesion: molecules and mechanics. *Science* **263**, 1720–1725.

Kim, R. Y. & Pagano, N. 1991 Crack initiation in unidirectional brittle-matrix composites. *J. Am. Ceram. Soc.* **74**, 1082–1090.

Koehler, J. S. 1970 Attempt to design a strong solid. *Phys. Res.* B **2**, 547–551.

Kwolek, S. 1968 South African Patent Application 6813051.

Lehoczki, S. L. 1978*a* Strength enhancement in thin-layered Al–Cu laminates. *J. Appl. Phys.* **49**, 5479–5485.

Lehoczki, S. L. 1978*b* Retardation of dislocation generation and motion in thin layered metal laminates. *Phys. Rev. Lett.* **41**, 1814–1818.

Manders, P. W., Chou, T. W., Jones, F. R. & Rock, J. W. 1983 Statistical analyses of multiple fracture in 0/90/0 glass fibre/epoxy resin laminate. *J. Mater. Sci.* **18**, 2876–2889.

Matthews, J. W. & Blakeslee, A. D. 1974 Defects in epitaxial multilayers. *J. Crystal Growth* **27**, 118–127.

McCartney, L. N. 1987 Mechanics of matrix cracking in brittle matrix fibre reinforced composites. *Proc. R. Soc. Lond.* A **409**, 324–350.

McCartney, L. N. 1992 Theory of stress transfer in a 0°–90°–0° cross ply laminate containing a parallel array of transverse cracks. *J. Mech. Phys. Solids* **40**, 27–68.

McLean, M. 1995 Nickel-base superalloys: current status and potential. *Phil. Trans. R. Soc. Lond.* A 351, 419–433.

Midwinter, J. E. 1984 Optical fibre communications, present and future. *Phil. Trans. R. Soc. Lond.* A **392**, 247–277.

Mileiko, S. T. 1969 The tensile strength and ductility of continuous fibre composites. *J. Mater. Sci.* **4**, 974–977.

Newkirk, M. S., Urquhart, A. W. & Zwicker, H. R. 1986 Formation of Lanxide™ ceramic composite materials. *J. Mater. Res.* **1**, 81–89.

Newnham, R. E. 1994 Non-mechanical properties of composites. In *Concise encyclopedia composite materials* (ed. A. Kelly), revised edn, pp. 214–220. Pergamon Press.

Parkhouse, J. G. & Kelly, A. 1996 The regular packing of fibres in three dimensions. (In preparation.)

Payne, D. N. & Gambling, W. A. 1975 Zero material dispersion in optical fibres. *Electron. Lett.* **11**, 176–178.

Penrose, R. 1974 The role of aesthetics in pure and applied mathematical research. *Bull. Inst. Math. Applics.* **10**, 266–271.

Perkins, J. 1986 Shape-memory effect alloys: basic principles. *Encyc. Mater. Sci. Engng* **6**, 4365–4368.

Prewo, K. M. 1982 A compliant, high failure strain, fibre reinforced glass matrix composite. *J. Mater Sci.* **17**, 3549–3563.

Pryce, A. W. & Smith, P. A. 1993 Matrix cracking in unidirectional ceramic matrix composites under quasi-static and cyclic loading. *Acta Metall. Mater.* **41**, 1269–1281.

Raj, R. 1993 Fundamental research in structural ceramics for service near 2000 °C. *J. Am. Cer. Soc.* **76**, 2147–2173.

Revcoleschi, A. & Dhalenne, G. 1993 Engineering oxide–oxide and metal oxide microstructures in directionally solidified eutectics. *Adv. Mater.* **5**, 657–662.

Riley, B. L. 1986 AV-8B/GR Mk 5 airplane composite applications. *Proc. Inst. Mech. Engrs* **200**, 1–17.

Ritter Jr, J. E. & Jakus, K. 1981 Fundamental approach to failure statistics of optical glass fibres. *J. Mater. Sci.* **16**, 1909–1912.

Roberts, S. S. J. & Davidson, R. 1991 Mechanical properties of composite materials containing embedded fibre optic sensors – fibre optic smart structures and skins. *SPIEE* **1588**, 1–16.

Roberts, S. S. J., Butler, R. J. & Davidson, R. 1992 In *Proc. 2nd European Conf. on Smart Structures and Materials* (ed. A. McDonach P. T. Gardiner R. S. McEwen & B. Culshaw), pp. 117–120. SPIE vol. 2361.

PHILOSOPHICAL TRANSACTIONS OF THE ROYAL SOCIETY A MATHEMATICAL, PHYSICAL & ENGINEERING SCIENCES

Rogers, A. J. 1988 Distributed optical fibre sensors for the measurement of pressure strain and temperature. *Phys. Rep.* **169**, 99–143.

Rogers, C. A. 1993 Smart material systems – the next logical step in composite technology. In *ECCM Smart Composites Workshop* (ed. P. Gardiner, A. Kelly, A. R. Bunsell), pp. 3–9. Abington, Cambridge: Woodhead.

Rogers, C. A., Barber, K. D., Bennett, K. D. & Wyn, A. 1988 Demonstration of a smart material with embedded actuators for active control. *SPIE* **986**, 90–105.

Rosenfield, A. R., Hahn, G. T., Bement Jr, A. L. & Jaffee, R. I. 1968 *Dislocation dynamics.* McGraw-Hill.

Schoutens, J. E. & Zorate, D. A. 1986 Structural indices in design optimization with metal–matrix composites. *Composites* **17** 188–204.

Sigalas, T., Kumosa, M. & Hull, D. 1991 Trigger mechanisms in energy-absorbing glass cloth/epoxy tubes. *Comp. Sci. Technol.* **40**, 265–287.

Talley, C. P. 1959 Mechanical properties of glassy boron. *J. Appl. Phys.* **30**, 1114–1115.

Talreja, R. 1987 *Fatigue of composite materials.* Lancaster Penna: Technomic.

Thomson, R. 1994 Fundamentals of fracture; a 1993 prologue and other comments. *Mater. Sci. Engng* A **176**, 1–7.

Thomson, R., Hsieh, C. & Rana, V. 1971 Lattice trapping of fracture cracks. *J. Appl. Phys.* **42**, 3154–3160.

Thornton, P. H. 1979 Energy absorption in composite structures. *J. Comp. Mater.* **13**, 247–262.

Thornton, P. H. & Edwards, P. J. 1982 Energy absorption in composite tubes. *J. Comp. Mater.* **16**, 521–545.

Tsai, S. W. & Hahn, H. T. 1980 *Introduction to composite materials.* Technomic.

Versnyder, F. L. & Shank, M. E. 1970 The development of columnar grain and single crystal high temperature materials through directional solidification. *Mater. Sci. Engng* **6**, 213–247.

Watt, W., Phillips, L. N. & Johnson, W. 1964 British Patent no. 1 110 791.

Yajima, S. 1980 Development of ceramics, specially silicon carbide fibres from organosilicon polymers by heat treatment. *Phil. Trans. R. Soc. Lond.* A **294**, 419–426.

Lecture held 6 April 1995

PHILOSOPHICAL TRANSACTIONS OF THE ROYAL SOCIETY A MATHEMATICAL, PHYSICAL & ENGINEERING SCIENCES

Figure 1. The Airbus A300-600, contains many components made of composites; the entire rudder and fin, engine cowlings, radome, large sections of the tailplane; the air brakes, spoilers, outer flap and wing tip, and undercarriage doors.

PHILOSOPHICAL TRANSACTIONS OF THE ROYAL SOCIETY A MATHEMATICAL, PHYSICAL & ENGINEERING SCIENCES

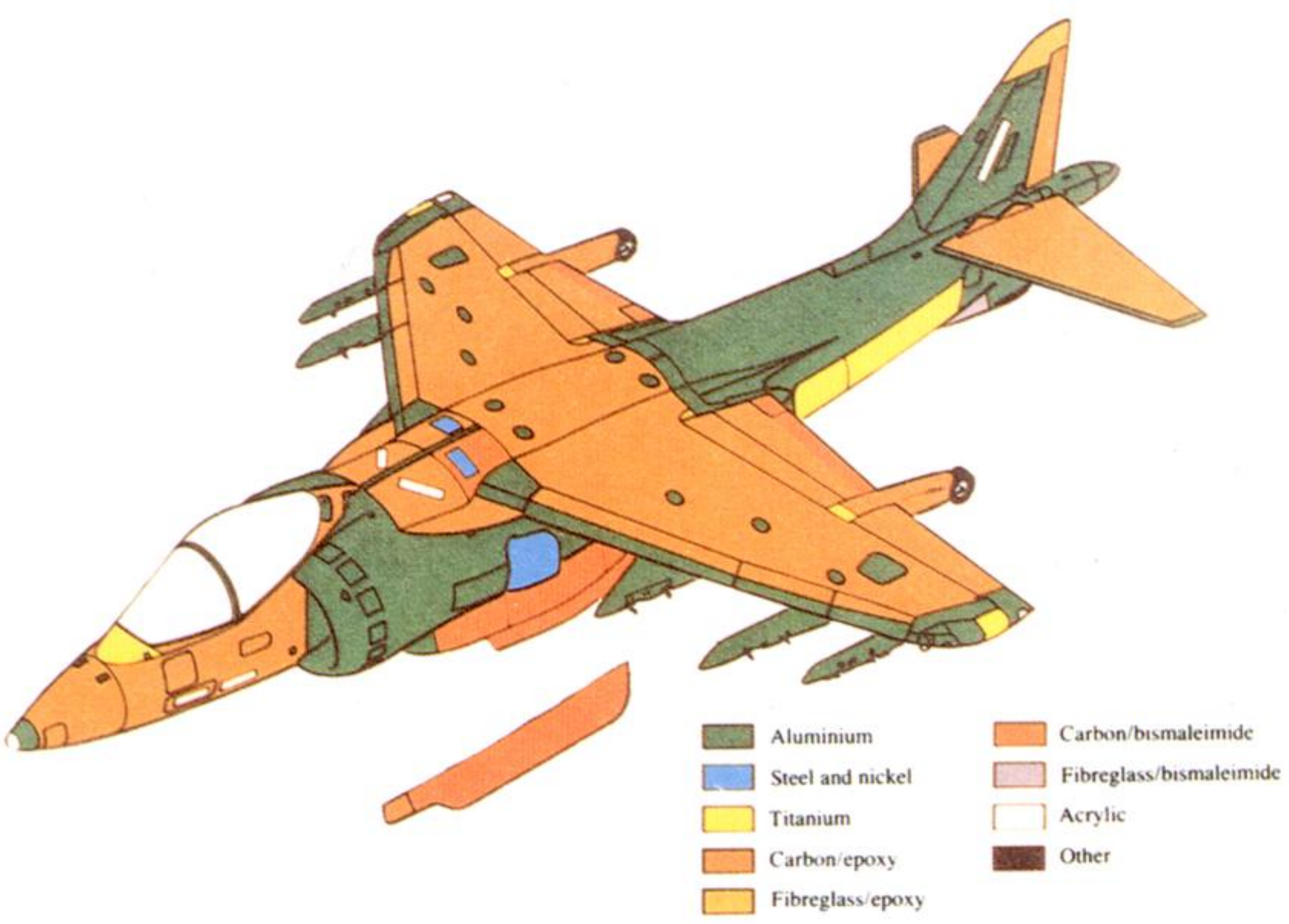

Materials usage

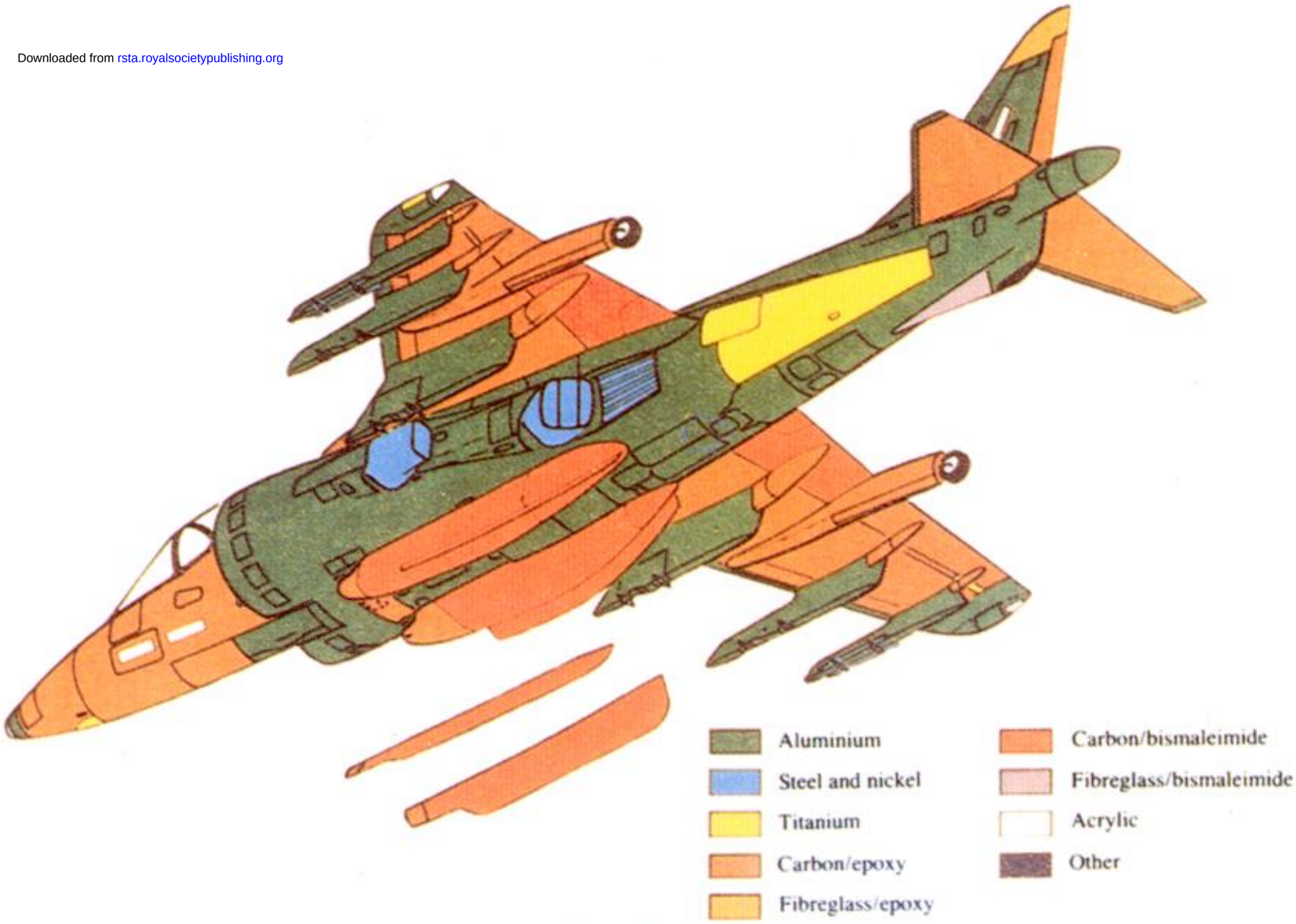

Materials usage

igure 2. The Harrier aircraft illustrating that many components are made of composites – multimaterials rather than single materials; from Riley (1986).

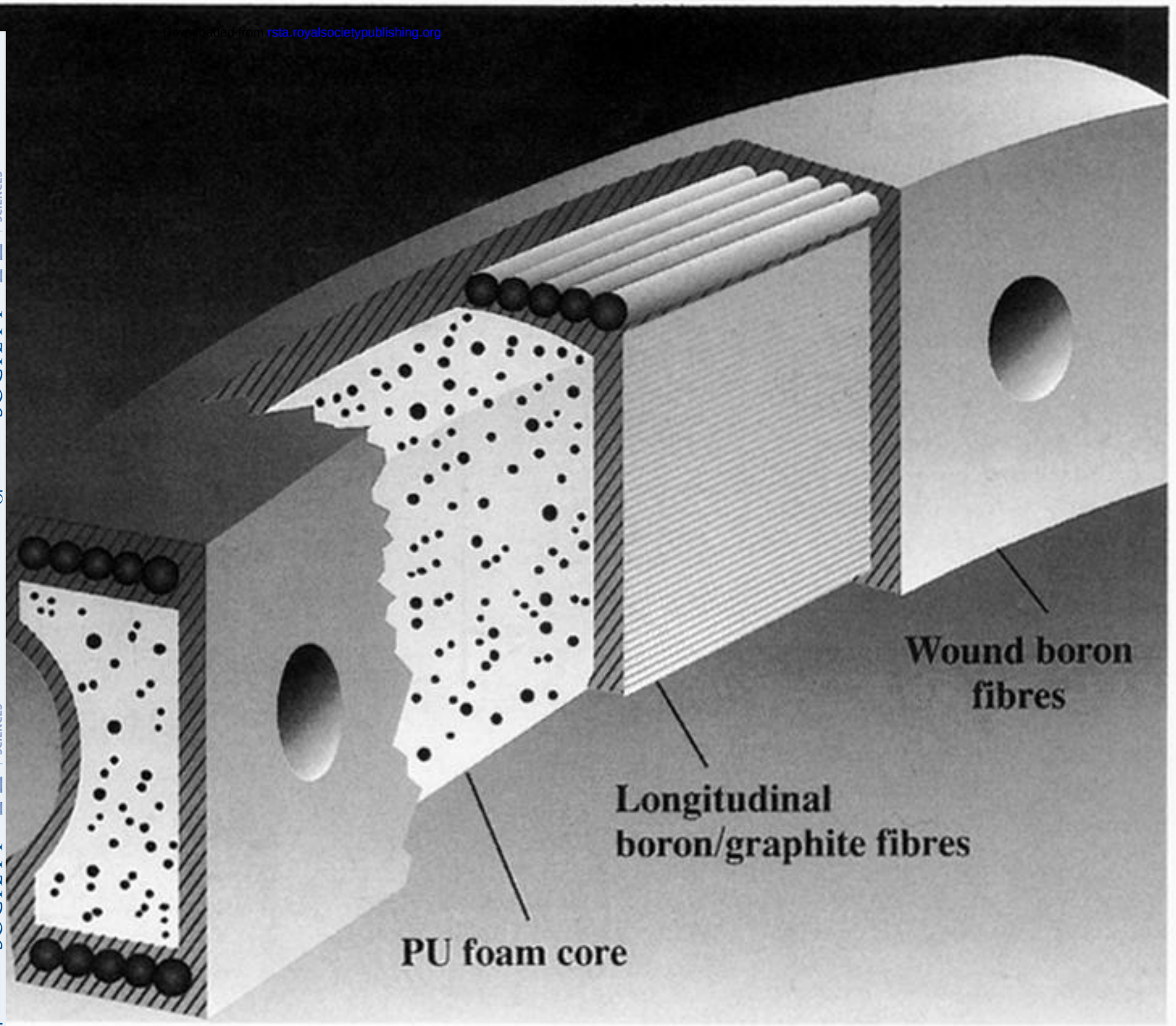

igure 3. Cross section of a modern high technology tennis racket.

PHILOSOPHICAL TRANSACTIONS OF THE ROYAL SOCIETY A MATHEMATICAL, PHYSICAL & ENGINEERING SCIENCES

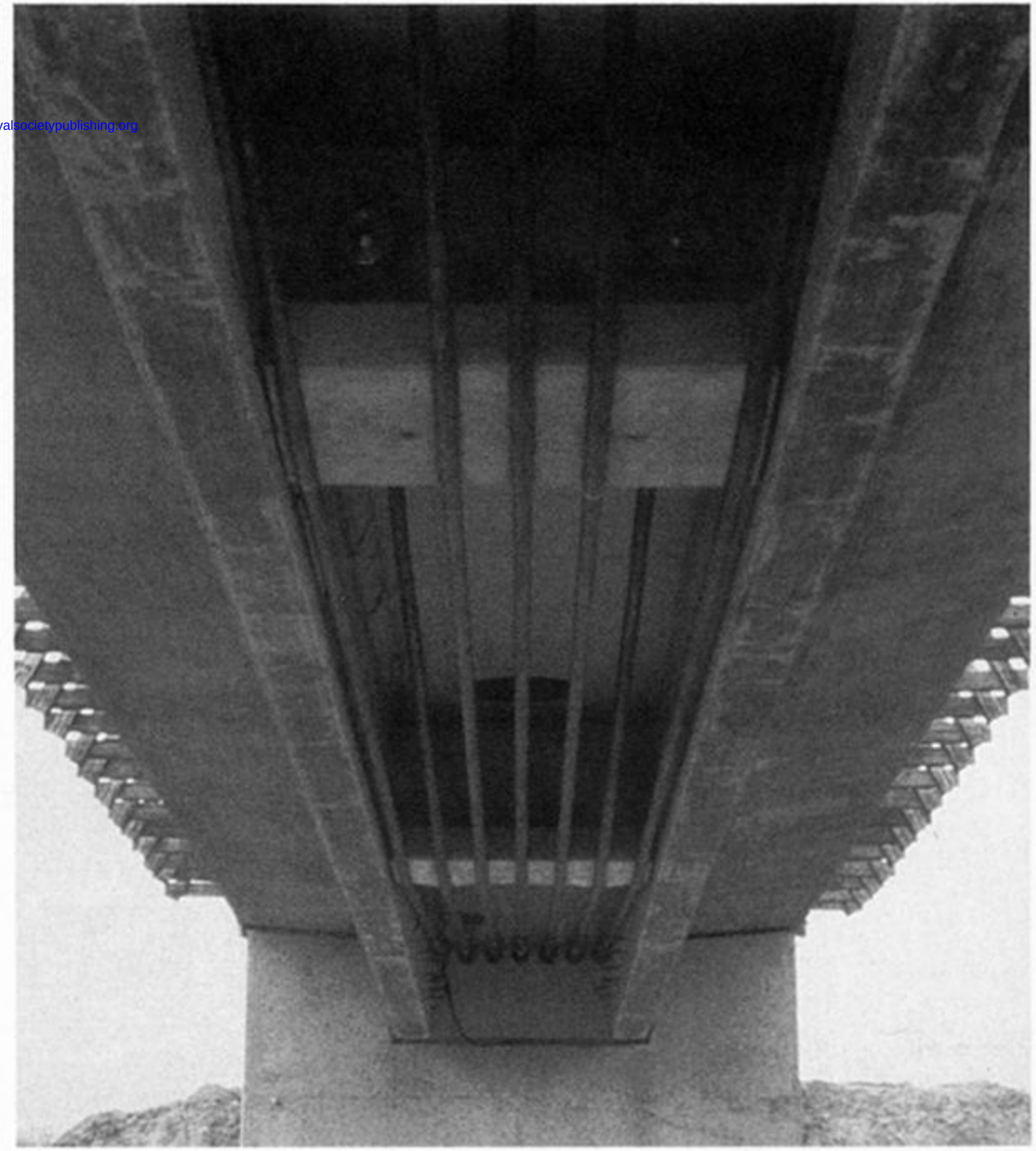

igure 4. The Marienfelde Bridge in Berlin showing the use of external grp reinforcing tendons.

PHILOSOPHICAL TRANSACTIONS OF THE ROYAL SOCIETY A MATHEMATICAL, PHYSICAL & ENGINEERING SCIENCES

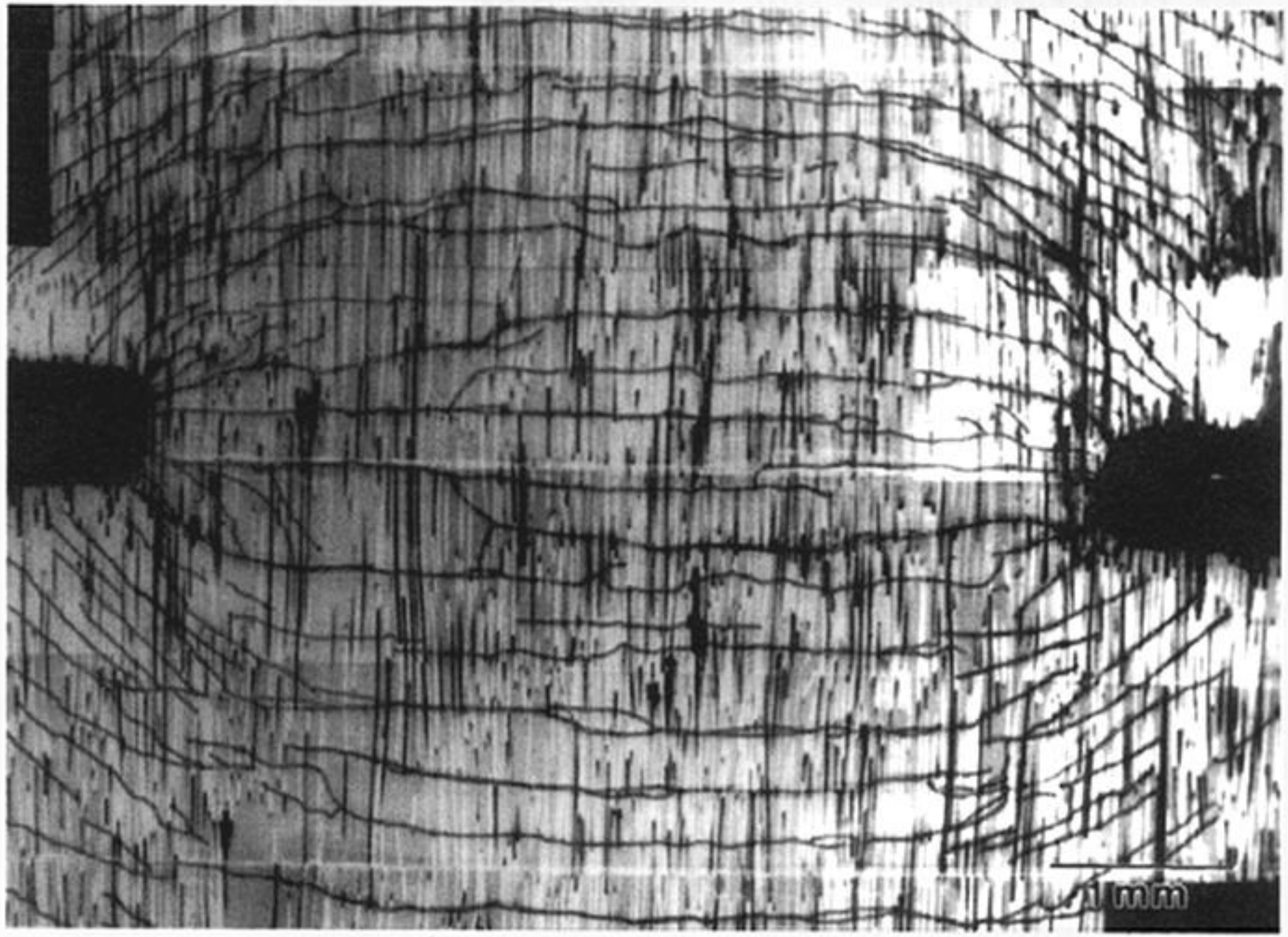

gure 12. Multiple cracking occurring between two notches in a laminated composite of 16 yers of 0°–90° lamellae each containing 40 vol.% of SiC fibres in a calcium aluminiosilicate ass matrix. Photograph courtesy Carl Cady.

PHILOSOPHICAL TRANSACTIONS OF THE ROYAL SOCIETY A MATHEMATICAL, PHYSICAL & ENGINEERING SCIENCES

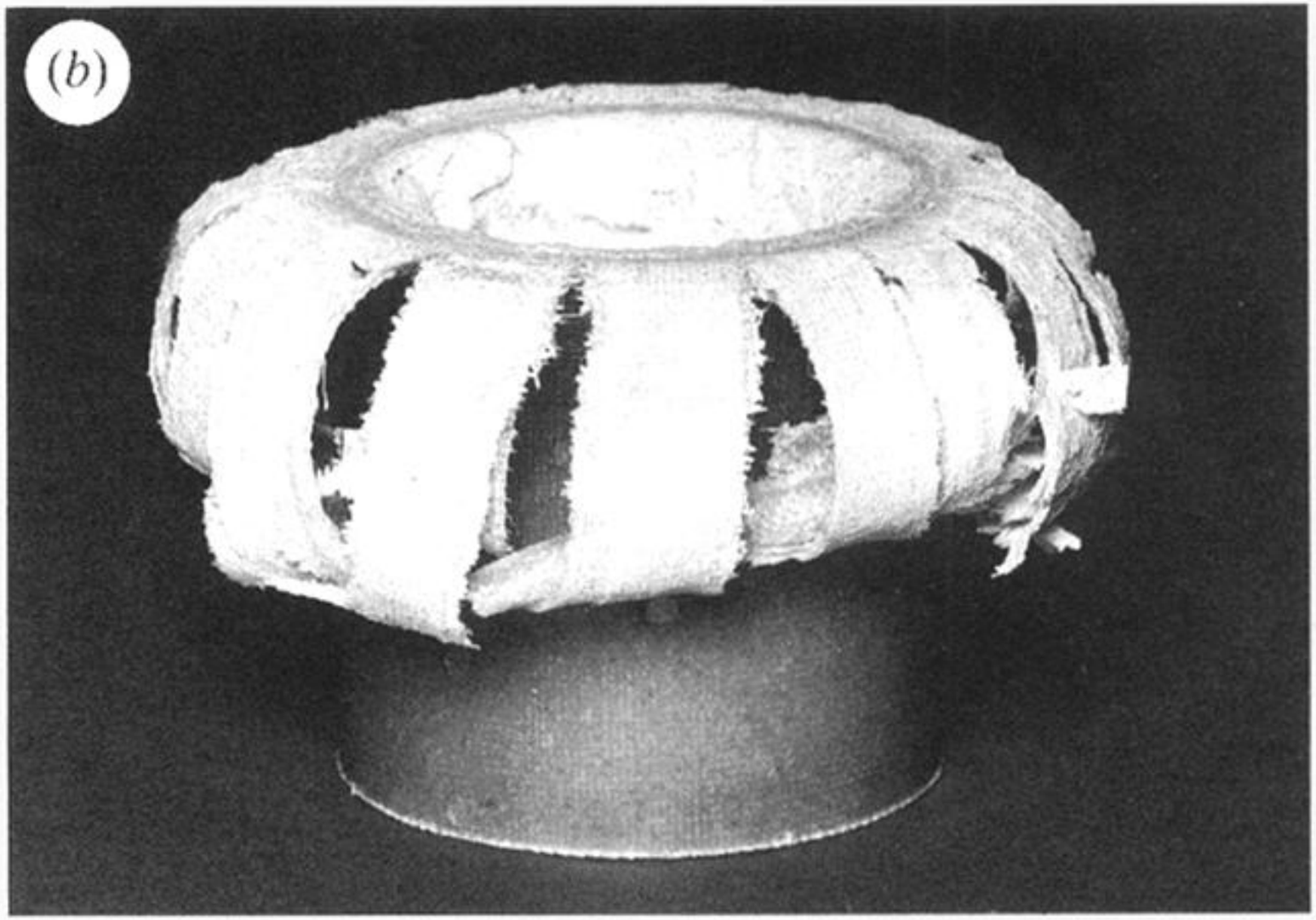

Figure 14. A comparison of crushed tubes of steel (a) and of woven glass cloth in epoxy resin (b) with $V_f \approx 0.54$. The tubes are each of 50 mm diameter and of about 2.5 mm wall thickness. Each was crushed at aboout the same speed. Photograph courtesy D. Hull.

PHILOSOPHICAL TRANSACTIONS OF THE ROYAL SOCIETY A MATHEMATICAL, PHYSICAL & ENGINEERING SCIENCES

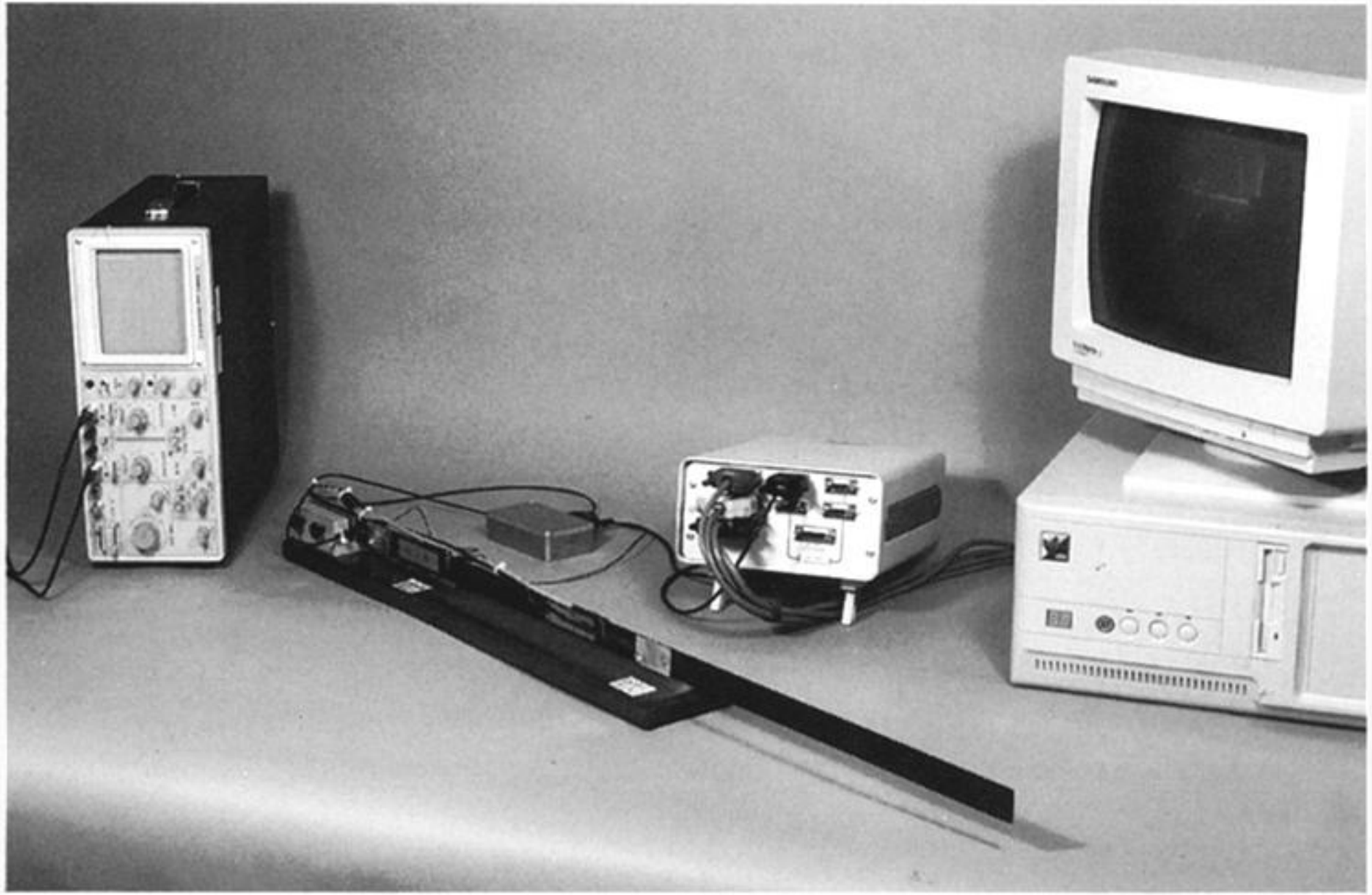

gure 20. A photograph of the experimental set up shown schematically in figure 19; from Roberts *et al.* (1994).